TRANSPORTATION POOLED FUND PROGRAM
QUARTERLY PROGRESS REPORT

Lead Agency (FHWA or State DOT): ____Maryland Department of Transportation____________

INSTRUCTIONS:
Project Managers and/or research project investigators should complete a quarterly progress report for each calendar quarter during which the projects are active. Please provide a project schedule status of the research activities tied to each task that is defined in the proposal; a percentage completion of each task; a concise discussion (2 or 3 sentences) of the current status, including accomplishments and problems encountered, if any. List all tasks, even if no work was done during this period.

Transportation Pooled Fund Program Project #	**Transportation Pooled Fund Program - Report Peric**
TPF-5(285)	■Quarter 1 (January 1 – March 31) □Quarter 2 (April 1 – June 30) □Quarter 3 (July 1 – September 30) □Quarter 4 (October 1 – December 31)

Project Title:		
Standardizing Lightweight Deflectometer Measurements for QA and Modulus Determination in Unbound Bases and Subgrades		
Name of Project Manager(s): Rodney Wynn	**Phone Number:** 443-572-5043	**E-Mail** RWynn@sha.state.md.us
Lead Agency Project ID: TPF-5(285)	**Other Project ID (i.e., contract #**	**Project Start Date:** January/15/2014
Original Project End Date: December/31/2015	**Current Project End Date:** December/31/2015	**Number of Extensions:** 0

Project schedule status:
□ On schedule □ On revised schedule □ Ahead of schedule ■ Behind schedule

Overall Project Statistics:

Total Project Budget	Total Cost to Date for Projec	Percentage of Work Completed to Date
$371,984	**$ 161,103.42**	**42%**

Quarterly Project Statistics:

Total Project Expenses and Percentage This Quarter	Total Amount of Funds Expended This Quarter	Total Percentage of Time Used to Date
$ 41,061.70 **11.0%**	**$ 41,061.70**	**52%**

Progress this Quarter (includes meetings, work plan status, contract status, significant progress, etc.):

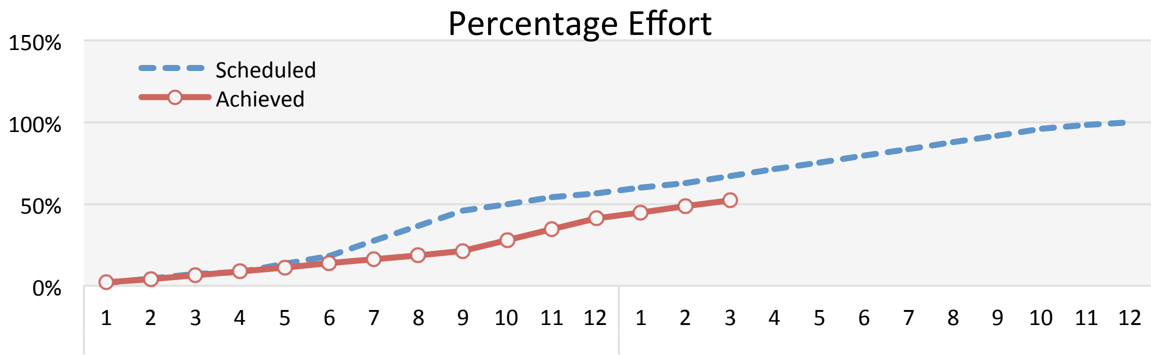

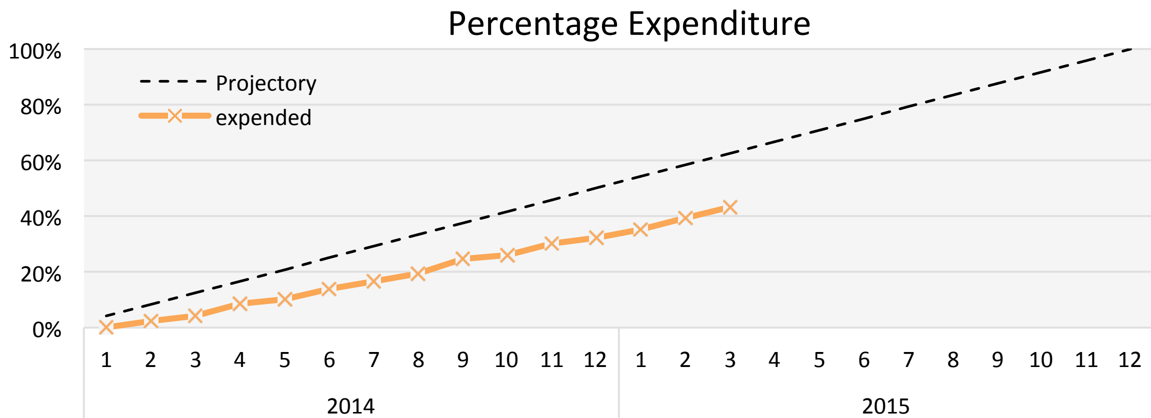

The progress with respect to each Task is as followed:

Literature Review (3.3% of the total effort). Percent completion of Task 1: 100%

The personnel continue the review of the current and upcoming literature when deemed necessary.

Project personnel participating in these activities: Schwartz, Khosravifar, Afsharikia.

Equipment Evaluation (2.4% of the total effort). Percent completion of Task 2: 100%

Model Refinement/Development (12.6% of the total effort). Percentage completion of Task 3: 86%
Several of the models refined/developed in Task 3 are in conjunction with laboratory efforts performed in Task 4.

Experimental models from Laboratory resilient modulus testing and LWD testing on Proctor mold.

Triaxial resilient modulus (M_R) tests performed in the laboratory using UTM-100 are not yet problem free. There are issues regarding the contact stress and oscillation of the load and deformation signals in very low stress/strain levels. We are constantly working with IPC and Instrotek to solve the problems and improve the data quality from the UTM-100. Details of the work is discussed in Appendix A.

The following specific work has been performed during the quarter:

(1) Triaxial M_R tests were performed according to AASHTO T-307 with and additional high stress loading intended to

match what is imposed by LWD tests on the Proctor mold.

(2) The MEPDG k1-k3 model was fit to the experimental data using the T-307 stress sequences. The quality of the fit was not acceptable on several tests, even on tests with high data quality. The reasons are being investigated

(3) The prediction of MEPDG k1-k3 model was poor when compared to the measured triaxial M_R at LWD stress levels. In other words, the model didn't work reliably beyond the range it was calibrated at.

(4) The prediction of MEPDG k1-k3 model was poor when compared to the measured LWD modulus on Mold (E-LWDmold). Part of the discrepancy is because of the need to assume Poisson's ratio assumption in E-LWDmold and because the E-LWDmold calculations includes both permanent as well as resilient deformations.

(5) The measured triaxial M_R at LWD stress levels had a good correlation with LWD modulus on Mold. However, the triaxial M_R was significantly higher than E-LWDmold. We believe that this is because of the permanent deformations in the LWD measurements.

Given the reasonable correlation between the measured E-LWDmold and the measured triaxial M_R, there is good potential for using LWD measurements during Proctor compaction curve testing to determine a reference value for field QA.

Beam Verification Tester

A frequency domain analysis of the LWD impact load on the Beam Verification Tester (BVT) was implemented in MATLAB. This step was performed to evaluate the full spectral response of different LWDs, find their static stiffness, and compare their inherent differences, which may lead to a systematic error in field. LWD tests using the three devices were conducted on BVT with varying spans. The static stiffness of the BVT was measured experimentally using an Instron machine.

The results suggested that contrary to Hoffman (2004), who found a significant difference between static stiffness and peak stiffness, the peak and static stiffness values are quite similar for the Dynatest LWD. Moreover, the peak stiffnesses for all LWDs were within 30% of the true stiffness of the beam. For the Olson LWD, the static stiffness calculated from spectral analysis was further from the true modulus of the beam. Some of the reasons for this were sensor overloading in the Olson LWD and the poor quality of load and deflection signals. Other potential reasons are still being investigated.

The most important outcome of the study was that the peak stiffness of all the three LWDs were in the same ballpark of the true static stiffness of the BVT and therefore there is no special need for the spectral analysis of the results. The details of the BVT work are provided in Appendix B.

Modeling Soil Drying

In this quarter, UNSAT-H was evaluated for its applicability to modeling the drying in soil. It became clear that the code is too complicated and impractical for use. The issues with UNSAT-H included (a) several required inputs, which might not be available during field construction and are not needed for our purposes and (b) the inability to trace the source of errors due to a non-user friendly interface.

As an alternative, we started working with the SVFlux and SVHeat models from SoilVision and the Flux code in Fortran77 (Wilson, 1990). Since the Flux code is old, it will likely require modification to be practically useful.

The results of these simulations will be compared with moisture drying trends of the 4 soils captured during the laboratory conditioning of specimens for LWD and resilient modulus testing during the drying process. An overview of this work is presented in Appendix C.

Project personnel participating in these activities: Schwartz, Khosravifar, Afsharikia.

Controlled Trials (18.8% of the total effort). Percentage completion of Task 4: 70%

Laboratory LWD tests on Proctor Compacted Specimens:
The process of LWD testing on Proctor molds were implemented on the soils obtained from the field projects right after compaction and during the drying process.

The LWD tests on the mold showed that the effect of short-term post-compaction moisture variation due to soil drying, which is one of the main variables during QA, is similar to the influence of compaction moisture content on modulus. This is a valuablefinding that simplifies the modeling of modulus as a function of compaction and post compaction moisture variations.

The Cary and Zapata (2010) environmental model was evaluated on the results. The default coefficients of the model did not provide a good prediction of measured values of moduli as a function of saturation level; however, the model coefficients could be optimized for each soil. This option will be evaluated on the test pits and field validations along with the original Cary and Zapata model.

In this quarter supplementary tests were also performed on granular aggregate base from the Georgia Avenue construction site to assess the effects of density, gravimetric moisture content, and volumetric moisture content on modulus in a more rigorous way. The results were in line with the findings of other researchers; degree of saturation impacts the modulus most significantly, but density is also important and at the same given degree of saturation higher density will result in higher modulus.

In addition, several lessons were learned regarding the best practice for performing LWD testing on the mold, especially with respect to Olson LWD. An important finding from our testing program was to be alert for sensor overloading; if necessary, the drop height should be reduced, especially when performing tests at wet of optimum.

The details of this work is provided in Appendix D.

Laboratory Resilient Modulus Tests:
Resilient modulus testing using the UTM-100 is not yet problem free. Even though the new setup (decoupling the loading shaft and load cell and using ball end connection between the two) has improved the LVDT and load signals significantly, there are still some issues regarding data acquisition and in fitting the k1-k3 model. We are constantly working with IPC and Instrotek to solve the problems and improve the data quality. The issues regarding the resilient modulus testing (Task 4) and modeling (Task 3) are explained in detail in Appendix A.

Controlled Soil Box Tests:
The literature review on the best types of in-situ sensors and the best practices for construction and data acquisition is being performed. The initial design of the test pits is shown in Appendix E.

Project personnel participating in these activities: Schwartz, Khosravifar, Afsharikia.

Field Validation (53.7% of the total effort). Percentage completion of Task 5: 25%

A web meeting was held on March 26 2015 to make arrangements with the technical advisory committee for the potential field projects in each state. A questionnaire was sent out to TAC for suitable field identification (Appendix F). So far, responses have been received from Florida, Indiana, and New York.

Draft Test Specifications (3.3% of the total effort). Percentage completion of Task 6: 0%

No progress was made on this task during the reporting period.

Workshop and Final Report (5.8% of the total effort). Percentage completion of Task 7: 2%

There is a workshop scheduled for June 2nd and 3rd at University of Maryland.

UMD personnel contact information:
Charles W. Schwartz- Principal Investigator, 301-405-1962, schwartz@umd.edu
Sadaf Khosravifar- GRA, 530-531-5030, sadafkh@umd.edu
Zahra Afsharikia- GRA, 202-747-4121, nafshari@umd.edu

Anticipated work next quarter:

- The continued monitoring and documentation of the literature. In particular, new papers presented at TRB 94th annual meeting will be reviewed.
- Task 3, 4, and 5 will be the main focus of the next quarter:
  1. Large pit tests
  2. Resilient modulus testing
  3. LWD Proctor testing with new modifications using Zorn LWD, Dynatest LWD, and Olson LWD.
  4. More rigorous investigation of field results using the laboratory resilient modulus and LWD measurements
  5. Model refinement: Drying, stress dependency, finite layer, spatial variability in the field
- On-site workshop

Circumstance affecting project or budget. (Please describe any challenges encountered or anticipated that might affect the completion of the project within the time, scope and fiscal constraints set forth in the agreement, along with recommended solutions to those problems).

The main difficulty affecting the project has been ongoing issues with resilient modulus testing machine.

Also, the sensor overload issues for the Olson LWD has hampered the testing program.

Potential Implementation:

LWDs should be implemented more widely and this should be done using standardized testing procedures and data interpretation methods. LWDs are a tool for performance based construction quality assurance testing, which not only results in a better product, but also provides the quantitative measures critical to better understanding the connection between pavement design and long term pavement performance. As the benefits of performance based quality assurance testing become increasingly apparent, more public agencies and private consultants are expected to acquire these tools and implement standardized procedures during their use. The product of this research will allow state DOT construction specifications to be modified to include this new light weight deflectometer (LWD) option during construction quality assurance.

Appendix A: Resilient Modulus Testing and Modeling

Laboratory resilient modulus testing using the UTM-100 is not yet problem free. Even though the new setup (decoupling the loading shaft and load cell) has improved the LVDT and load signals significantly, there are still some issues regarding data acquisition and fitting the k1-k3 model. We are constantly working with IPC and Instrotek to solve the problems and improve the data quality.

A. Data quality

There is an oscillation in the system, the source of which has not yet been found. Potential causes of the oscillation are as followed:

a. Grounding issues: The electrician has measured the voltage from ground to the surface and there is no potential voltage or earth leakage. The electrician is in the process of connecting an earth lead from the CDAS to the Loading Frame to assure the system is fully grounded.
b. Turbulence within the oil in the hydraulic system. Oil flow through both the actuator and the servo valve may create turbulence within the oil.
c. Internal friction of the seals and actuator bushings as well as the mass of the ram and loading shaft may cause delays in control which will appear as hunting or oscillation of the load, which will be most evident at very low loading forces.

The UTM-100 system components are designed to withstand and control high loads at full capacity and the unit is now running at very low end of its range. Even though the load cell has been changed, the control circuit (Servo valve and Actuator) are still components critical to its operation and these are designed to operate at up to 100kN.

A potential solution would be to use a smaller capacity loading and control frame such as a UTM25.

This oscillations are more pronounced at lower load levels and lower deformations and have caused the following problems in the recorded data:

1. Contact stress.
   The tolerance of contact stress according to AASHTO T-307 is 10%+/- 0.7kPa. The achieved contact stress in our system is approximately about 14% and above the tolerance due to the oscillation. Figures 1 and 2 illustrate this problem. There have been efforts to improve the signal by changing the PID parameters. The loading waveshape has significantly improved by adjusting the PID parameters and putting the ball end connection between the load cell and loading shaft. However, there is still interference during the rest period and satisfactory results are not yet achieved.

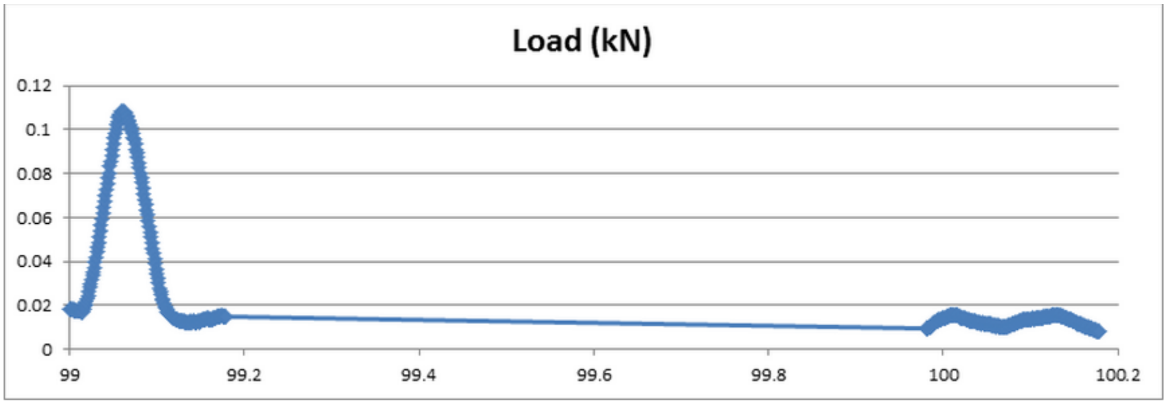

Figure 1. Wave shape for sequence 1 (13.8kPa Axial Stress, 12.4kPa Cyclic Stress, 1.4kPa Contact Stress of SP-SM soil

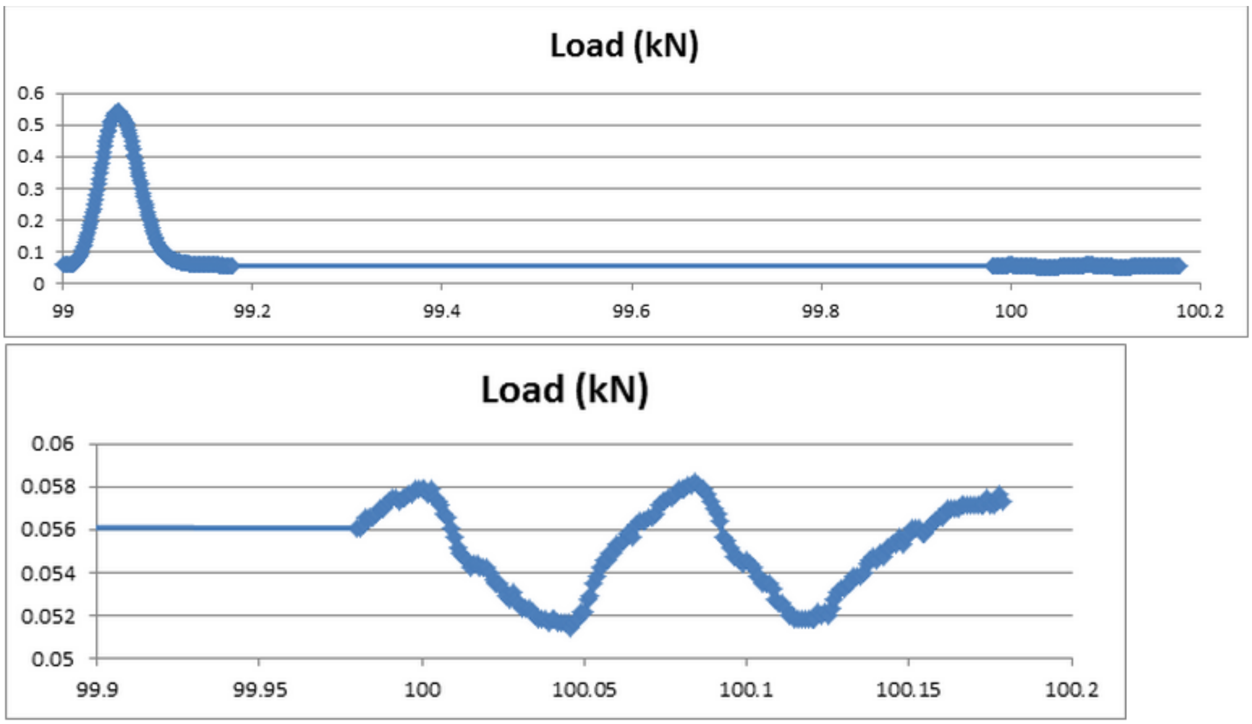

Figure 2. Waveshape for Sequence 15 (68.9kPa Axial Stress, 62kP Cyclic Stress, 6.9 kPa Contact Stress) for SP-SM soil. The lower graph is a magnified view of the response late in the rest period.

2. Oscillation of load and deformation wave shapes for stiffer materials.
   The oscillation gets worse on stiffer material. The interference that is observed during the rest period on the softer samples now becomes part of the loading signal in the firmer samples. Switching to Base/Subbase stress levels and adjusting the PID values improves the signals but not enough to obtain satisfactory wave shapes. It is difficult to determine what is going on but it may just be the UTM-100 is not responsive enough to apply smaller deformations as the material becomes stiffer. The hydraulic system is not designed for the lower levels of its 100KN capacity.

3. Data analysis and fitting the k1-k3 model

For SP-SM material right after compaction, the shape of loading and deformation signals look good, as shown in Figures 1 and 2 with slight oscillation during the rest period. The standard deviation between the M_R of the last 5 cycles at each sequence was less than 2%, showing high quality data acquisition. However, the R^2 values after fitting the k_1-k_3 model were low. The predicted versus measured modulus for SpSm03 sample right after compaction is shown in Figure 3.

Table 1 shows the fitting parameters for three specimens right after compaction and after 18 to 25 hours of drying. On average, the modulus increased by approximately a factor of 7 while the MC decreased about 6%. The load and deformation waves hapes were poor on the tests performed 'after drying' as compared to the 'at-compaction' data due to the higher stiffness of the material. Switching to the Base/Subbase procedure improved the quality of data to some extent. The solution to this problem is still being investigated. It is important to note that the fitting of the data was done after removing the test sequences with higher than 10% coefficient of variation between cycles, which was the case for the stiffer samples.

Table 1. Resilient Modulus test results for SPSM

SP-SM		SpSm01		SpSm02		SpSm03	
Pa	[kPa]	101.3	101.3	101.3	101.3	101.3	101.3
k1	[-]	624.6	4546.9	614.0	5520.3	690.6	3576.9
k2	[-]	0.2	0.4	0.2	0.5	0.1	0.3
k3	[-]	0.0	-0.5	0.0	-0.8	0.0	-0.4
SSE	$[MPa]^2$	228.7	1435.9	471.5	43670.8	385.8	4710.1
Sqr(SSE)	[MPa]	15.1	37.9	21.7	209.0	19.6	68.6
R^2	[-]	0.6	0.9	0.4	0.8	0.2	0.8
R^2_adj	[-]	0.5	0.9	0.2	0.8	0.0	0.7
MC@Compaction	[%]	8.86	8.86	7.94	7.94	8.52	8.52
MC@Testing	[%]	8.86	2.92	7.94	2.89	8.52	2.49
S@Compaction	[%]	110.6	110.6	115.9	115.9	119.5	119.5
S@testing	[%]	110.6	36.4	115.9	42.2	119.5	34.9
Drying interval	[hr]	0	18	0	21	0	25
Drying temperature	[°C]	-	25	-	25	-	25
Drying relative humidity	[%]	-	50%	-	50%	-	50
Dry Density	[kg/m3]	2174.22	2174.22	2230.58	2230.58	2216.82	2216.82
Compaction effort	[-]	Stnd	Stnd	Mod	Mod	Mod	Mod

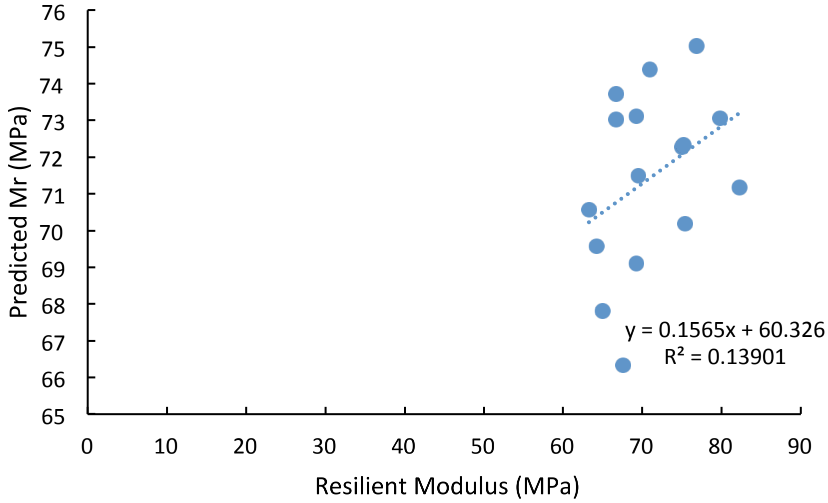

Figure 3. SpSm03 tested right after compaction. Testing MC = 8.5%. This is an example of good quality data but a very poor fit. Constraining or not constraining the k parameters did not affect the quality of the fit significantly

For the SC soil the fits were of of better quality right after compaction as well as after drying.

Table 2. Resilient Modulus test results for SC

		SC01		SC02		SC03	
Pa	[kPa]	101.30	101.30	101.30		101.30	101.30
k1	[-]	1168.70	4547.09	1339.10		1365.08	2132.98
k2	[-]	0.47	-0.08	0.56		0.45	0.28
k3	[-]	-2.65	-0.34	-3.50		-3.06	-0.23
SSE	$[MPa]^2$	242.44	21299.40	461.76		328.11	448.49
Sqr(SSE)	[MPa]	15.57	145.94	21.49		18.11	21.18
R2	[-]	0.93	0.36	0.93		0.94	0.98
R2_adj	[-]	0.91	0.12	0.90		0.93	0.97
MC@Compaction	[%]	12.0%	12.0%	12%	12%	11.9%	11.9%
MC@Testing	[%]	12.0%	6.4%	12%	7.9%	11.9%	9.7%
S@Compaction	[%]	85%	85%	94%	94%	93%	93%
S@testing	[%]	85%	45%	94%	61%	93%	76%
Drying interval	[hr]	0	24	0	22	0	18
Drying temperature	[C]	-	25	-	25	-	25
Drying relative humidity	[%]	-	50	-	50	-	50
Dry Density	[kg/m3]	1940.6	1940.6	1986.3	1986.3	1992.9	1992.9
Compaction effort	[-]	Stnd	Stnd	Stnd	Stnd	Stnd	Stnd

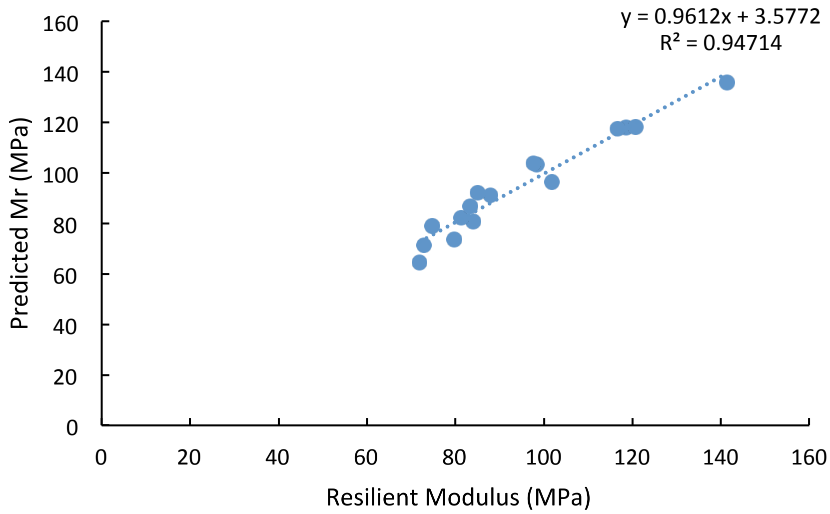

Figure 4. SC03 tested right after compaction. Testing MC= 12%. This is an example of good quality data and fit.

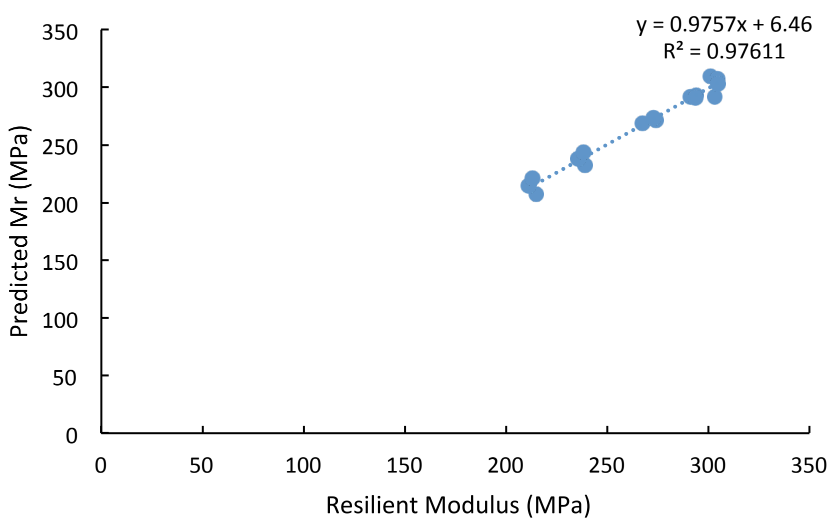

Figure 5. SC03 tested after 18 hours drying- Testing MC = 9.7%. This is an example of good quality data and fit.

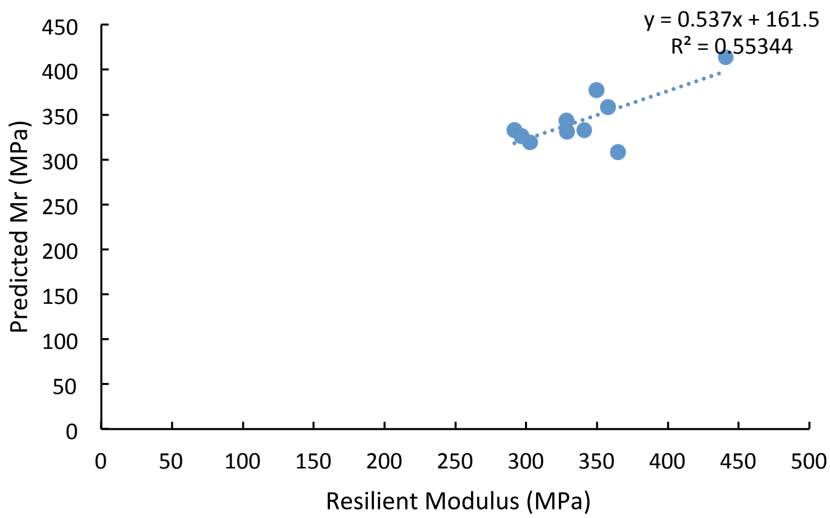

Figure 6. SC01 tested after 24 hours drying- Testing MC = 6.4%. This is an example of low quality data and fit.

The specimens were also tested at a higher stress level close to that imposed by LWD drops on the Proctor mold in the laboratory experiments (Explained in detail in the previous QPR).

The two objectives from this task were:

1. To investigate whether the k1-k3 stress dependent model is capable of predicting modulus at higher stress levels close to that imposed by LWD.
2. To investigate whether the resilient modulus measured at LWD stress level in the triaxial apparatus is comparable to the LWD modulus performed on top of the proctor molds.

Unfortunately, the fitted models were not capable of predicting modulus at LWD stress levels and significantly underestimated the modulus. Moreover, the k1-k3 model was not capable of predicting LWD modulus measurements on the mold. Figure 5 shows the comparison of the measured and predicted modulus after compaction and after 20 hrs of drying for SC soil, which had the highest quality of resilient modulus data.

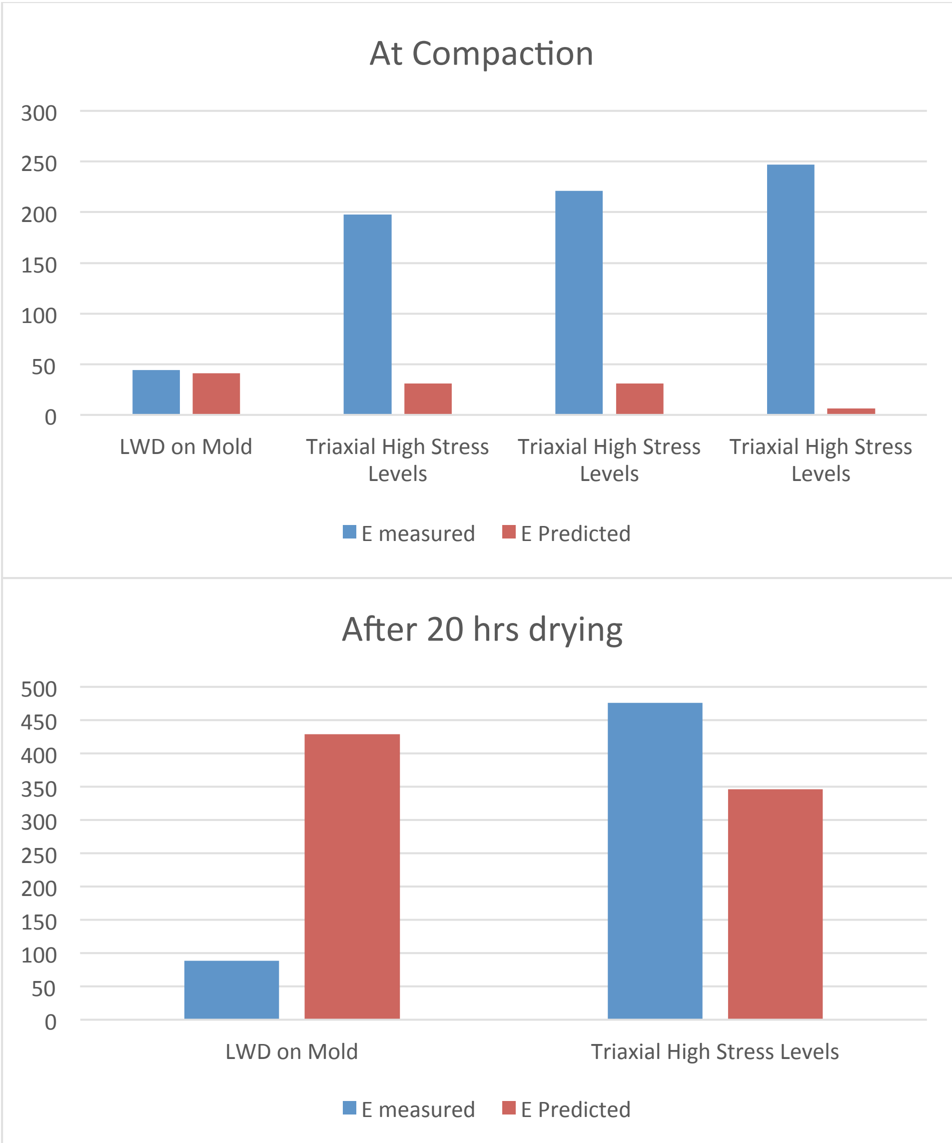

Figure 7. SC soil predicted modulus based on the models.

The measured modulus from the triaxial test at LWD on mold stress levels (M_R –TX) were not in close numerical agreement with the LWD modulus on mold (E-LWD). However, there was a good correlation between the two. The comparison of the two moduli for four different types of soils are presented in Figure 8 and Table 3.

The differences in the magnitude of the two measured moduli may be attributed to the differences in stress states (despite the efforts to simulate similar stresses in the two tests), the assumed Poisson's ratio in E-LWD interpretation, and, most importantly, the fact that in calculation of E-LWD is based on the total strain while M_R –TX only considers only the resilient part of the deformation.

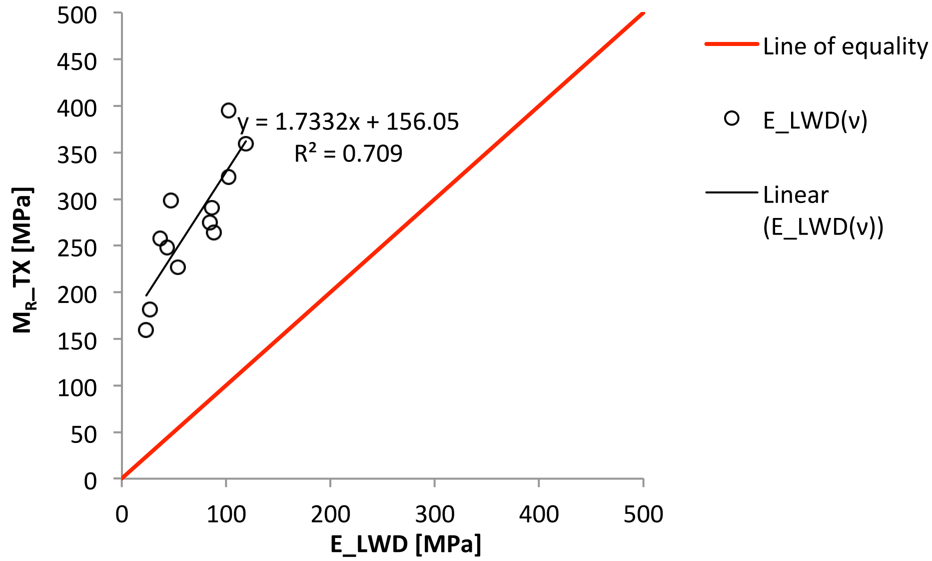

Figure 8. Triaxial M_R (M_R-tx) vs LWD modulus for the 4 evaluated soils

Table 3. Measured resilient modulus test at LWD stress level from the triaxial test (M_R- tx) and E_LWD for the four soils after compaction, 8 hours drying after compaction and 24 hours drying after compaction

		v	MR-tx	E_LWD(v)
		[-]	[Mpa]	[Mpa]
GW	@comp	0.22	159.9	34.4
	@8hrs	0.21	181.4	36.3
	@24hrs	0.20	298.6	60.6
SP-SM	@comp	0.38	258.1	36.9
	@8hrs	0.38	275.3	84.3
	@24hrs	0.38	323.4	102.3
SM	@comp	0.42	226.8	53.5
	@8hrs	0.40	290.8	86.1
	@24hrs	0.38	395.2	102.1
SC	@comp	0.42	247.8	43.3
	@8hrs	0.40	263.8	87.9
	@24hrs	0.38	359.5	118.8

Overall, this good correlation between the two tests can assist us in setting the right target modulus in the field.

Appendix B: Beam Verification Tester

The performance of the three LWD devices was examined with the beam verification tester (BVT) developed by Hoffman et al. (2004)

The span of the beam was changed from 40 cm to 70 cm in 10 cm intervals to provide a linear elastic response with different ranges of stiffness values. The static stiffness of the beam was also experimentally measured by applying a ramp load at a slow rate of 0.2mm/sec using an Instron loading machine.

The beam stiffness under the LWD drop was calculated using two methods:

1. Peak stiffness (k_p). Using the conventional method of peak load and peak deflection as reported by the LWD.
2. Static Stiffness (k_s). Based on the frequency response function and the assumption of a single-degree-of-freedom mechanical model.

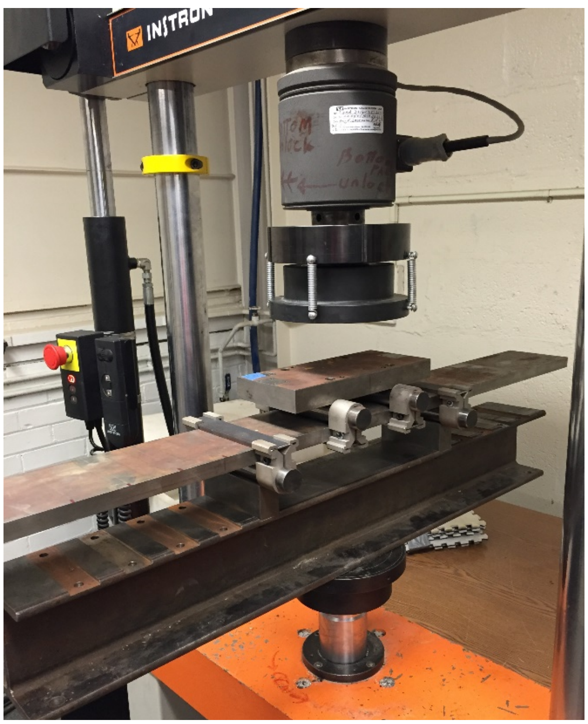

Figure 9. BVT under Instron machine

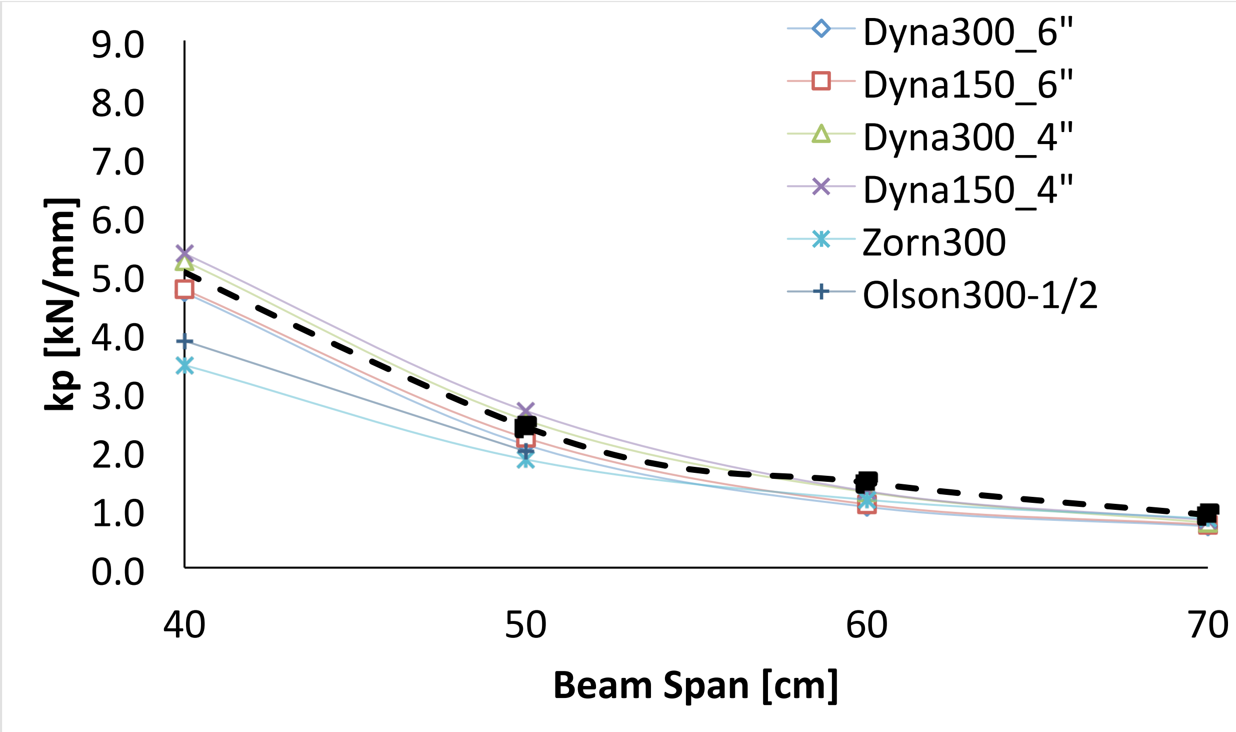

Figure 10. K_P as a function of beam span for the all the evaluated devices.

Dynatest LWD: Tests were performed using 150 mm and 300 mm plates. The 10 kg weight was dropped from 10 cm (4”) and 15 cm (6”) heights. Full height drops were not possible due to overloading the sensors. The Dynatest LWD provides error message in this case. The k_p results were in line with true k_s of the beam at all beam spans. The k_s from spectral analysis yielded results close to k_p.

Olson LWD: Tests were performed using 150, 200, and 300 mm plate sizes. The weight was dropped from full height. The k_p from Olson was not in line with the true stiffness of the beam. After analyzing the data it was found that the deflection sensor reached its range limit (explained in more detail in Appendix D). The tests were performed again for half height drops on 40 cm and 50 cm spans. The k_p underestimated the true stiffness of the beam. The k_s from spectral analysis underestimated the true modulus of the beam even further. The investigations on the Olson device are still ongoing.

Zorn LWD: Tests were performed using a 300 mm plate. The tests were performed from the full height of the device. When decreasing the beam span (at 40 and 50 cm), occasional “sensor overload” messages were received. K_p results were in line with true k_s of the beam at beam spans 60 and 70 cm. As the beam span decreased, the k_p underestimated the stiffness. This could be attributed to the assumed load of 7.07 kN on Zorn LWD. Based on Dynatest and Olson load measurements, the applied load increases as the beam gets stiffer (shorter spans).

Overall, contrary to Hoffman (2004) it was found that the conventional peak-based method of backanalysis produces correct estimates of the static stiffness of the BVT. The spectral-based data interpretation method could enhance the results marginally for Dynatest but was deficient for Olson LWD.

Samples of the spectral analysis on Dynatest and Olson LWD are as followed:

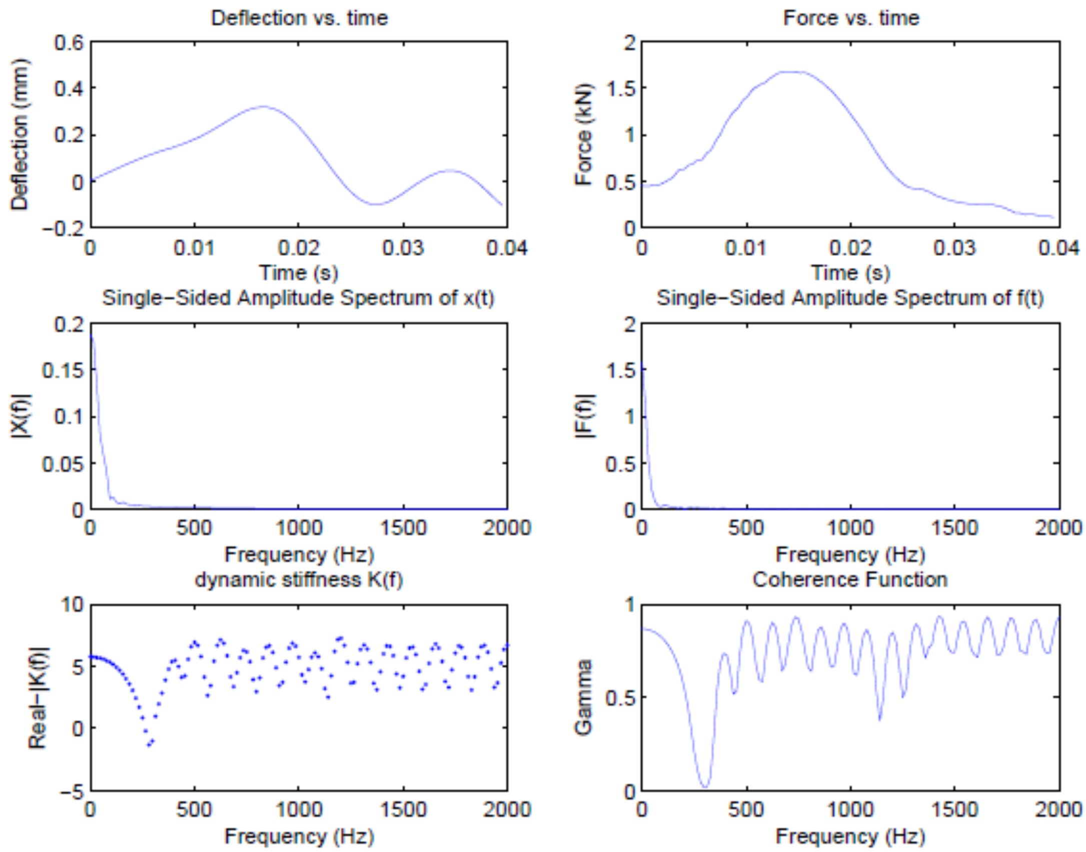

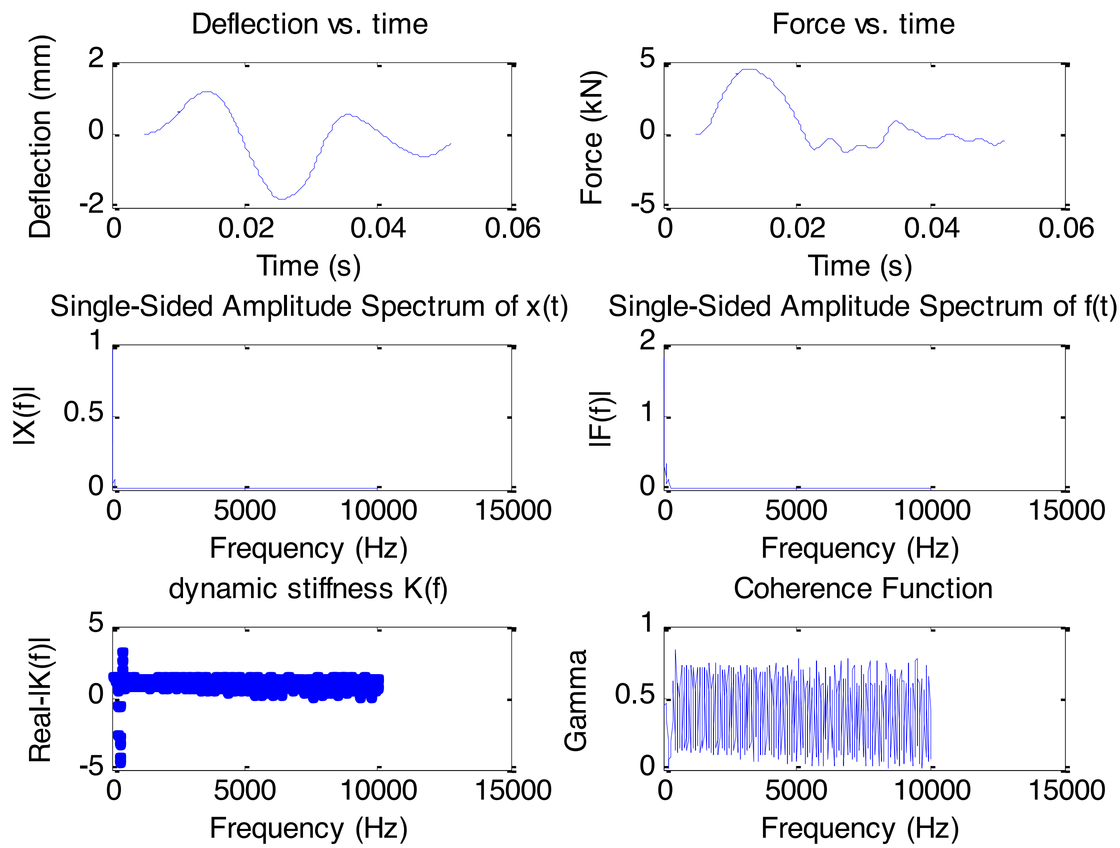

Span [cm]	ks [kN/mm]	Zorn 300 [kN/mm]	Dyna 300_6" [kN/mm]	Dyna 150_6" [kN/mm]	Dyna 300_4" [kN/mm]	Dyna 150_4" [kN/mm]	Olson 300 [kN/mm]	Olson 200 [kN/mm]	Olson 150 [kN/mm]	Olson 100 [kN/mm]	Olson 300-1/2 [kN/mm]	Prima100 Hoffmann [kN/mm]
70	0.9	0.834	0.707	0.732	0.767	0.810	2.158	2.234				3.400
60	1.5	1.159	1.038	1.082	1.288	1.305	2.227	2.245	2.252	2.172		2.670
50	2.4	1.848	2.099	2.215	2.519	2.678	2.462	2.451			1.982	2.170
40	5.0	3.457	4.693	4.748	5.234	5.360	3.603				3.872	
30	7.9											

Zorn 300 [kN/mm]	Dyna 300_6" [kN/mm]	Dyna 150_6" [kN/mm]	Dyna 300_4" [kN/mm]	Dyna 150_4" [kN/mm]	Olson 300 [kN/mm]	Olson 200 [kN/mm]	Olson 150 [kN/mm]	Olson 100 [kN/mm]	Olson 300-1/2 [kN/mm]	Prima100 Hoff/hammer [kN/mm]
-7%	-21%	-19%	-15%	-10%	140%	148%				278%
-20%	-28%	-25%	-11%	-10%	54%	55%	55%	50%		84%
-23%	-13%	-8%	5%	12%	3%	2%			-17%	-10%
-31%	-6%	-5%	5%	7%	-28%				-23%	

Appendix C. Flux 1D and SoilVision

Flux code is a 1D finite element package that was written by Wilson (1990) in his PhD thesis to solve the explicit finite difference solution for the coupled soil-atmosphere system. The modified Penman method used to estimate the evaporation was renamed Wilson-Penman method. Wilson verified the numerical model by comparing the measurements from of actual evaporation of a sand column under controlled laboratory condition in his PhD thesis.

The SoilVision software is a commercial product that models the coupled heat and vapor flux in the soil. It includes as an analysis example the sand column model from Wilson's thesis (Figure 11).

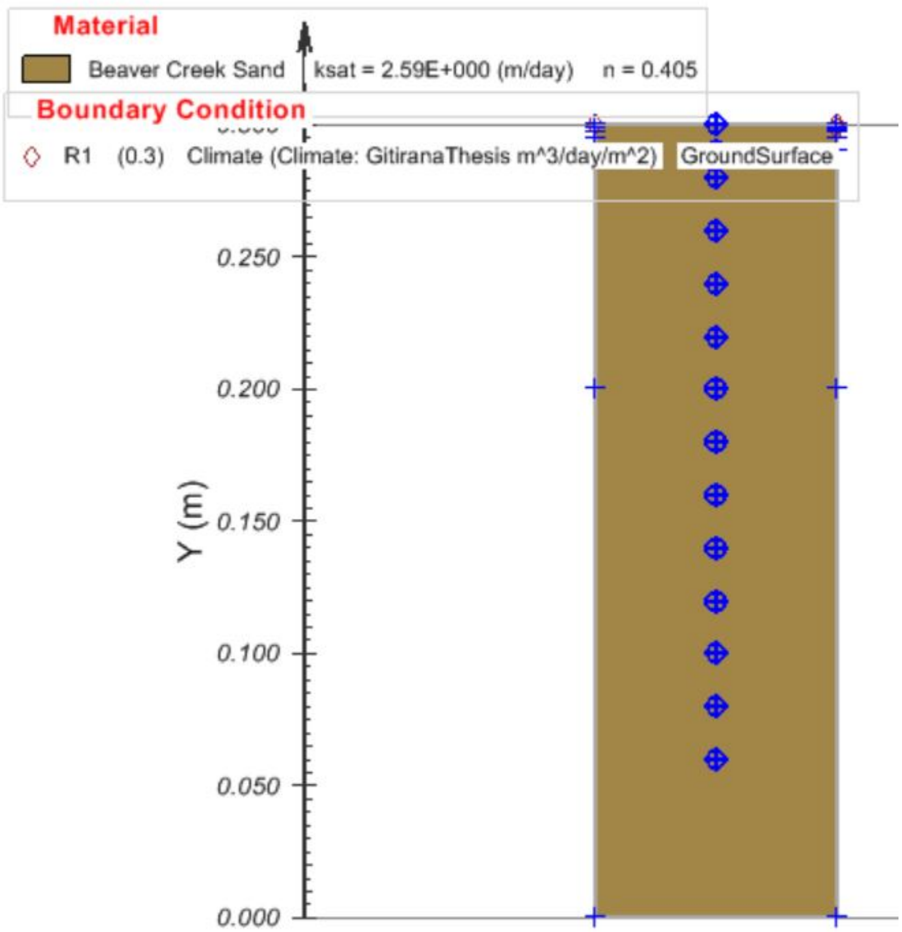

Figure 11. Wilson soil column example model provided with the SoilVision software.

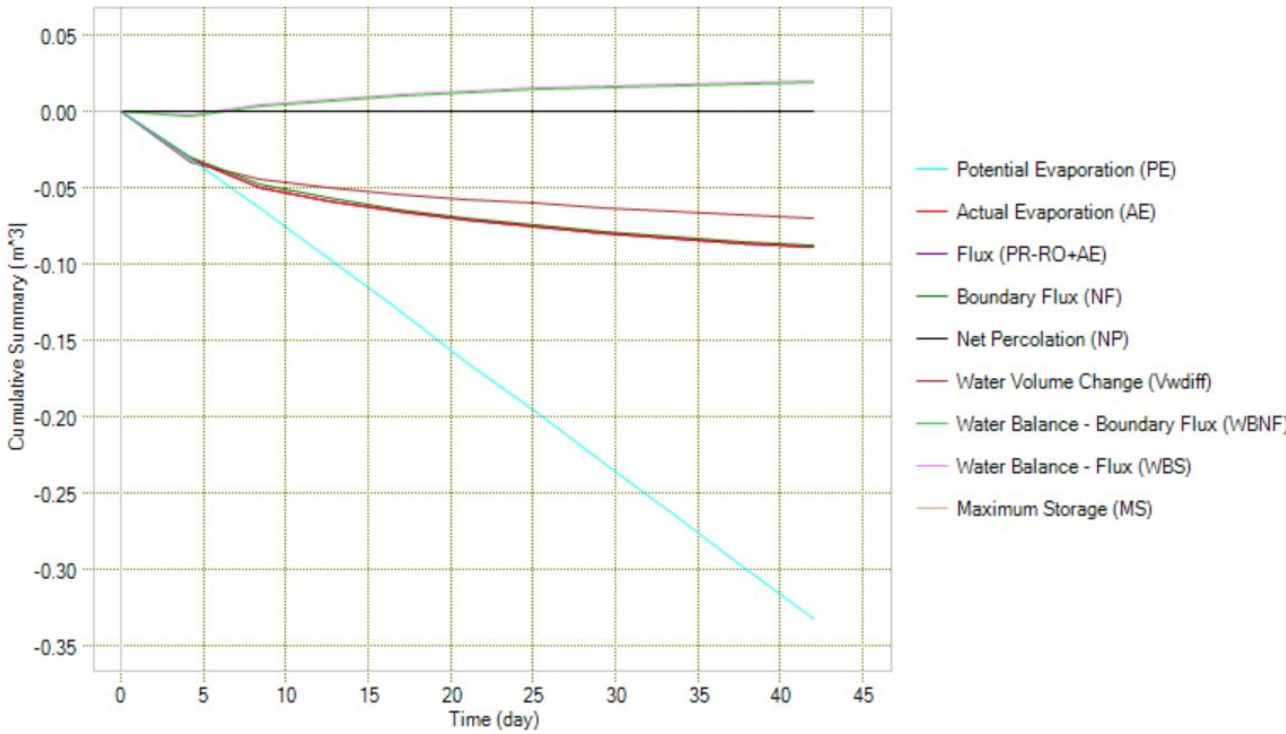

Figure 12. Cumulative summary of simulated Wilson sand column test in SoilVision's SVFlux and SVHeat.

Figure 12 shows a cumulative summary for the simulated Wilson sand column in SoilVision for a time period of 42 days. The potential and actual evaporation are in good agreement for the first 4 days.

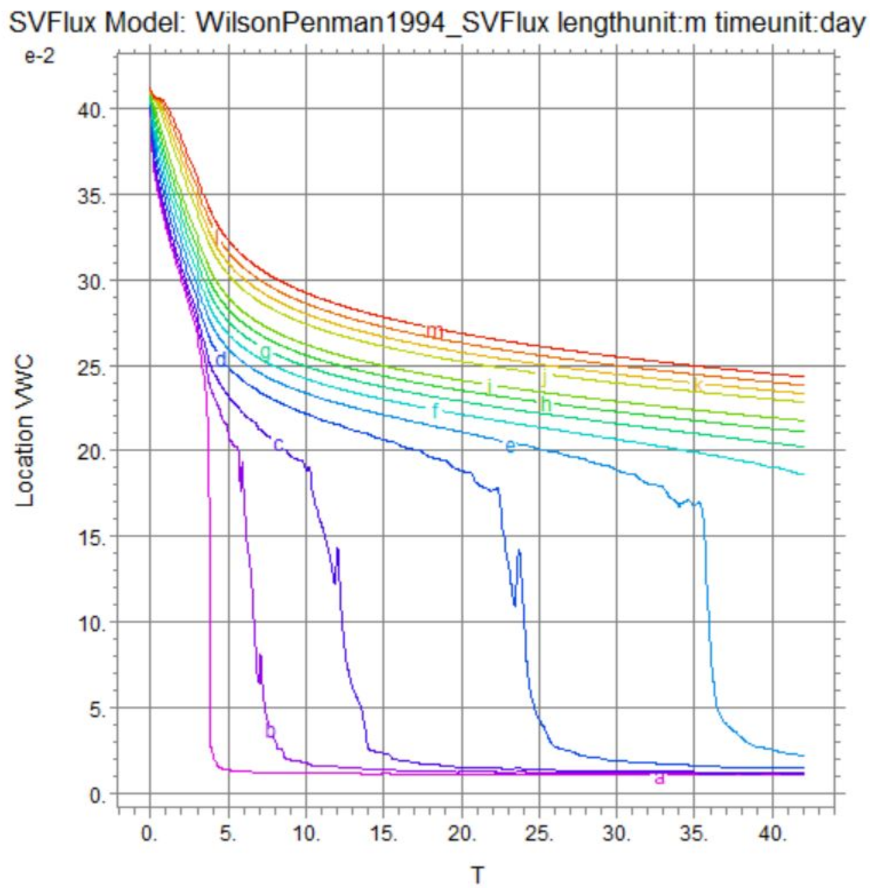

Figure 13. Volumetric water content change vs. depth for simulated Wilson sand column test in SoilVision's SVFlux and SVHeat

Figure 13 shows the change in volumetric water content for Wilson's soil column at all the node locations as simulated by SoilVision. As expected, the nodes that are closer to the surface of the column experience more loss in volumetric water content.

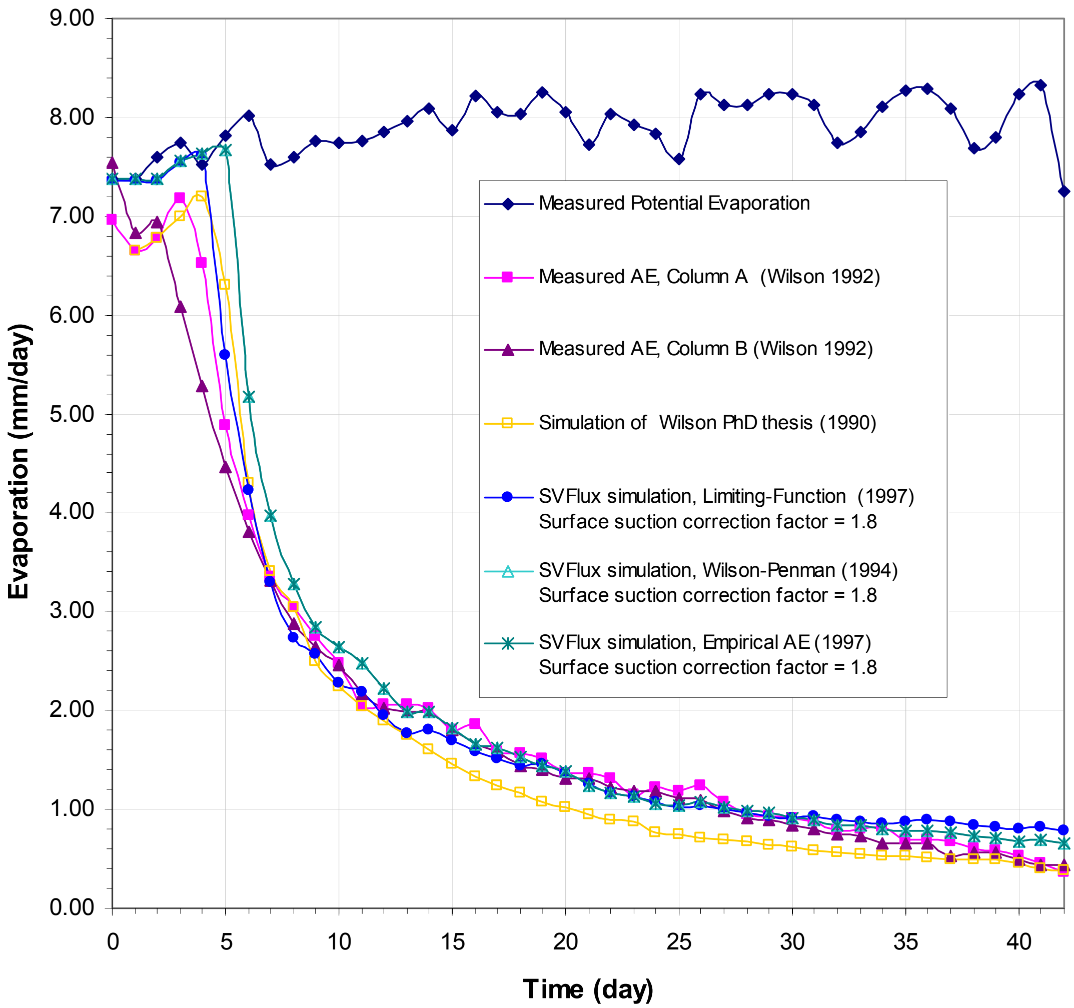

Figure 14. Comparison of evaporation simulated using SVFlux with laboratory data and numerical results by Wilson (1990) (Figure 23 from the SVFlux verification manual).

According to Figure 14, during the first 24 hours the SVFlux simulation predicts that the actual evaporation is essentially equal to the Potential Evaporation. However the Flux code predicts this more accurately.

Appendix D: Laboratory Experiments – LWD Tests on Mold

Lessons Learned from Tests Performed on LWD Molds Using the Olson LWD-1.

The Olson-LWD 1 is still under development and is not yet commercialized. The software for analyzing the full duration of the signals was received after performing LWD tests on Proctor molds and therefore could only be used for post-mortem analyses and interpretations.

A thorough analysis of the results showed that in several tests there were problems regarding the force and/or velocity signals.

Force Signal:

The force signal was "clipped" in several tests, meaning that the signal amplitude (voltage) entering the data acquisition system was higher than the system can handle. The indication of clipping on the NDE-360 is the "% Scale" value in the lower left during data acquisition (Figure 15). The % scale value is a measure of the amount of dynamic range of the acquisition system that is being used and should be kept between 10 and 85 percent to avoid losing data or "clipping".

The reason for the clipped force signal was a higher gain set on the force channel during the data acquisition (x10). For the subsequent measurements, it is recommended that the gain on the force channel be set to x1 unless the signal is too weak to trigger the system.

Olson Instruments Inc. is also going to use more sensitive sensors for the force channel in their commercialized version of LWD and then fix the gain at x1. Olson Instruments is also working to improve the software in this regard to make it more user-friendly and have the software provide warnings when data is out of the physical range of the sensor.

The clipped force resulted in an approximately 10% underestimation of the load and consequent stiffness on several measurements.

Fortunately, a strong relationship was found between the peak load and peak deflection using only the unclipped data, as shown in Figure 22. The relationship was used to correct the clipped peak loads on the affected cases.

Deformation Signal:

The deformation recorded by the geophone was inaccurate in several cases due to either clipping or mechanically bottoming the geophone sensor. To avoid the clipping issue in the future, the gain should be set at x1 except for very stiff material.

The mechanical bottoming the geophone sensor is hard to determine from the signal due to the integration. But if the measured deflection is greater than 3.0 mm (or 0.120 inches), the geophone will be nearing its mechanical limit. This issue had affected data recorded on SC, SM, and SC-SM soils at wet of optimum (Figure 23). There is no way to correct these tests. For subsequent LWD tests on Proctor molds using the Olson LWD, the LWD weight should be dropped from a lower height.

Data from a test on SC soil at wet of optimum are shown in Figure 15 to Figure 21 (File name = SLYCY4). Figure 15 shows the monitor of NDE-360 monitor. The plots of the signals during the test present the filtered data which may obscure the fact that the data is clipped.

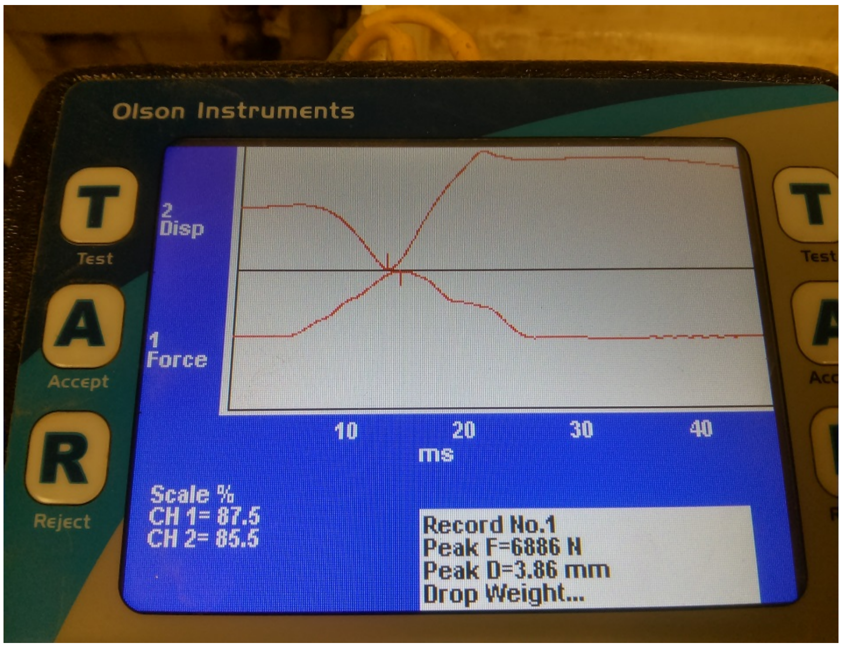

Figure 15. SLYCY4- Drop#1 screen shot of NDE-360 Olson Instruments data acquisition. The plotted graphs show the data after filtering.

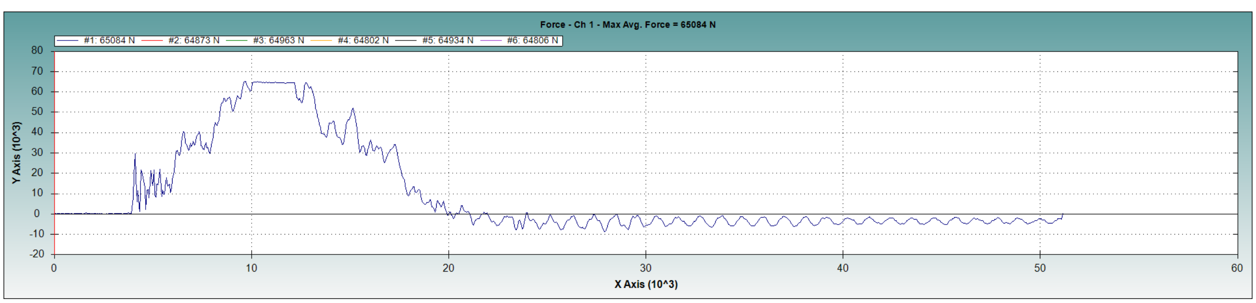

Figure 16. Clipped load signal before filtering. Data from SLYCY4- Drop#1.

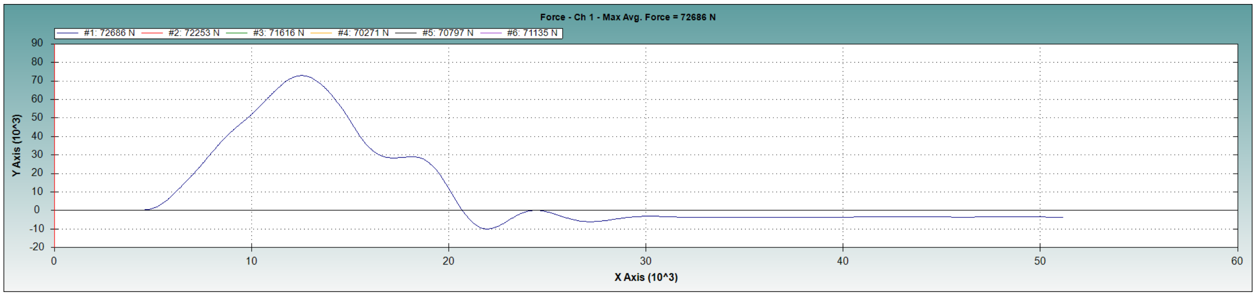

Figure 17. Clipped load signal after filtering. Filtering has masked the clipping in data. Data from SLYCY4-Drop#1.

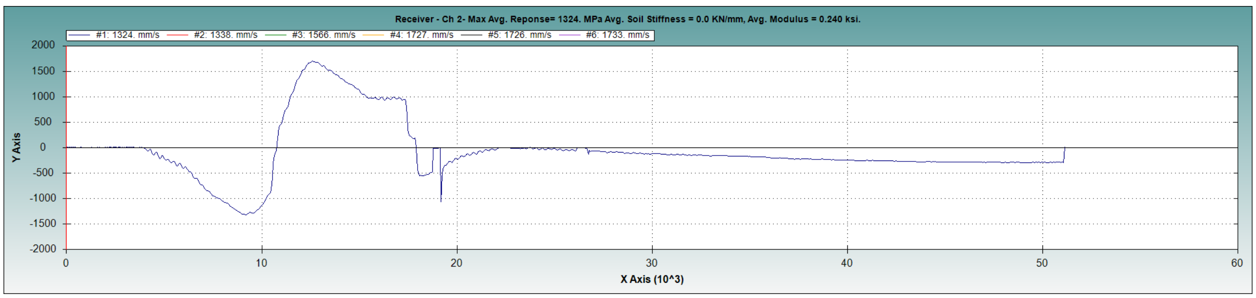

Figure 18. Velocity signal before filtering. This signal is very close to being clipped. Data from SLYCY4-Drop#1.

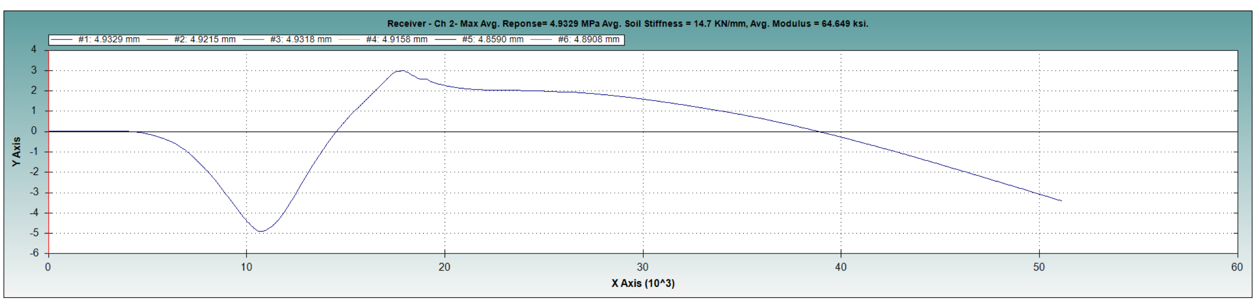

Figure 19. Integrated deflection signal. Data from SLYCY4- Drop#1.

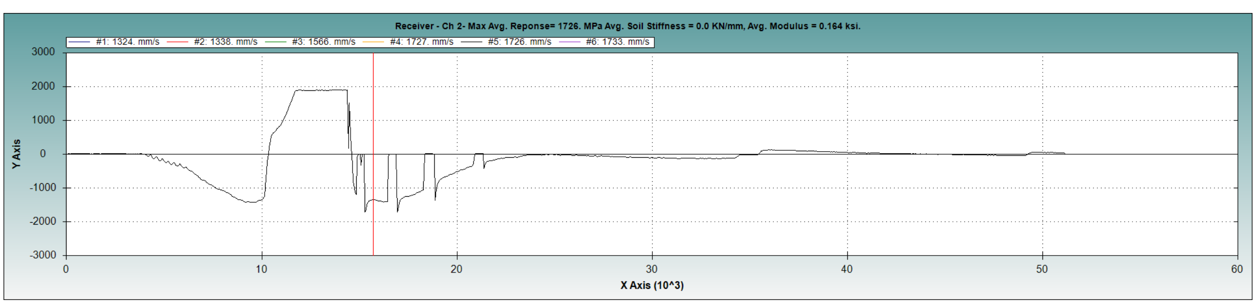

Figure 20. Velocity signal before filtering. This signal is clipped. Data from SLYCY4- Drop#5.

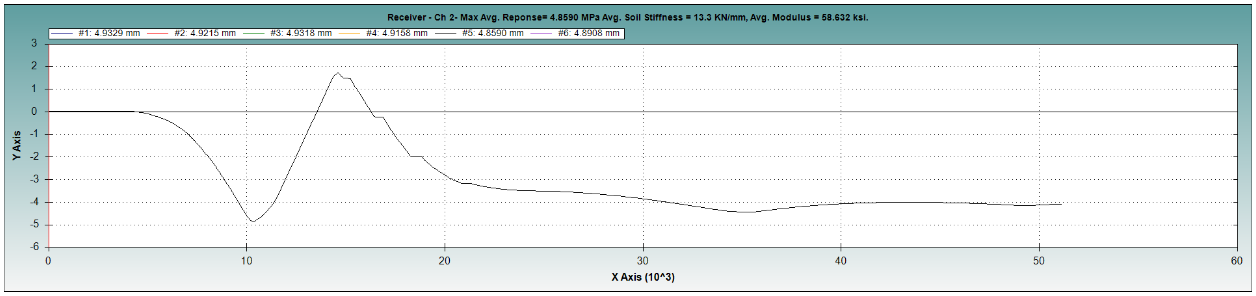

Figure 21. Integrated deflection signal. The deflection seems normal while the velocity had been clipped. Data from SLYCY4- Drop#5.

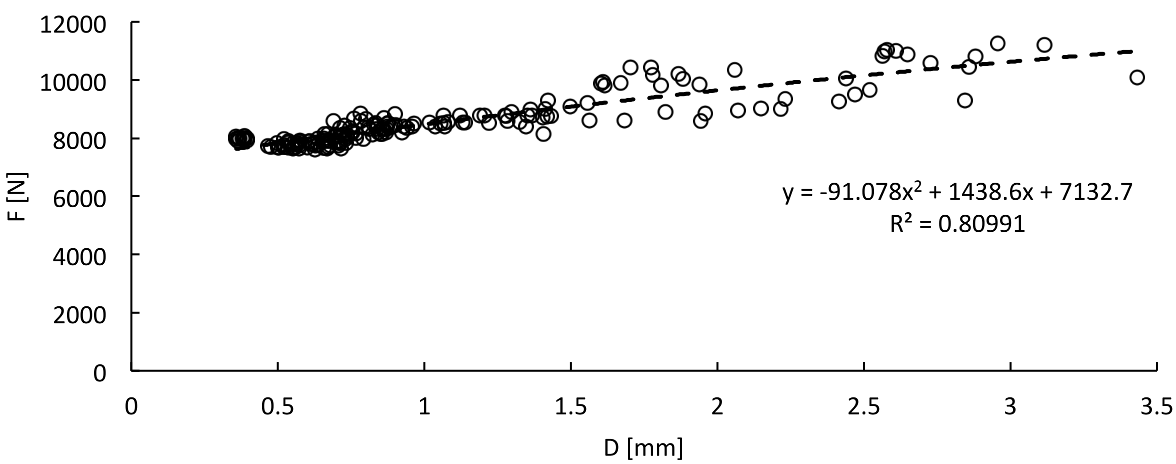

Figure 22. Force vs. Deflection for Olson LWD measurements on the four evaluated soils, used to correct the clipped peak load data.

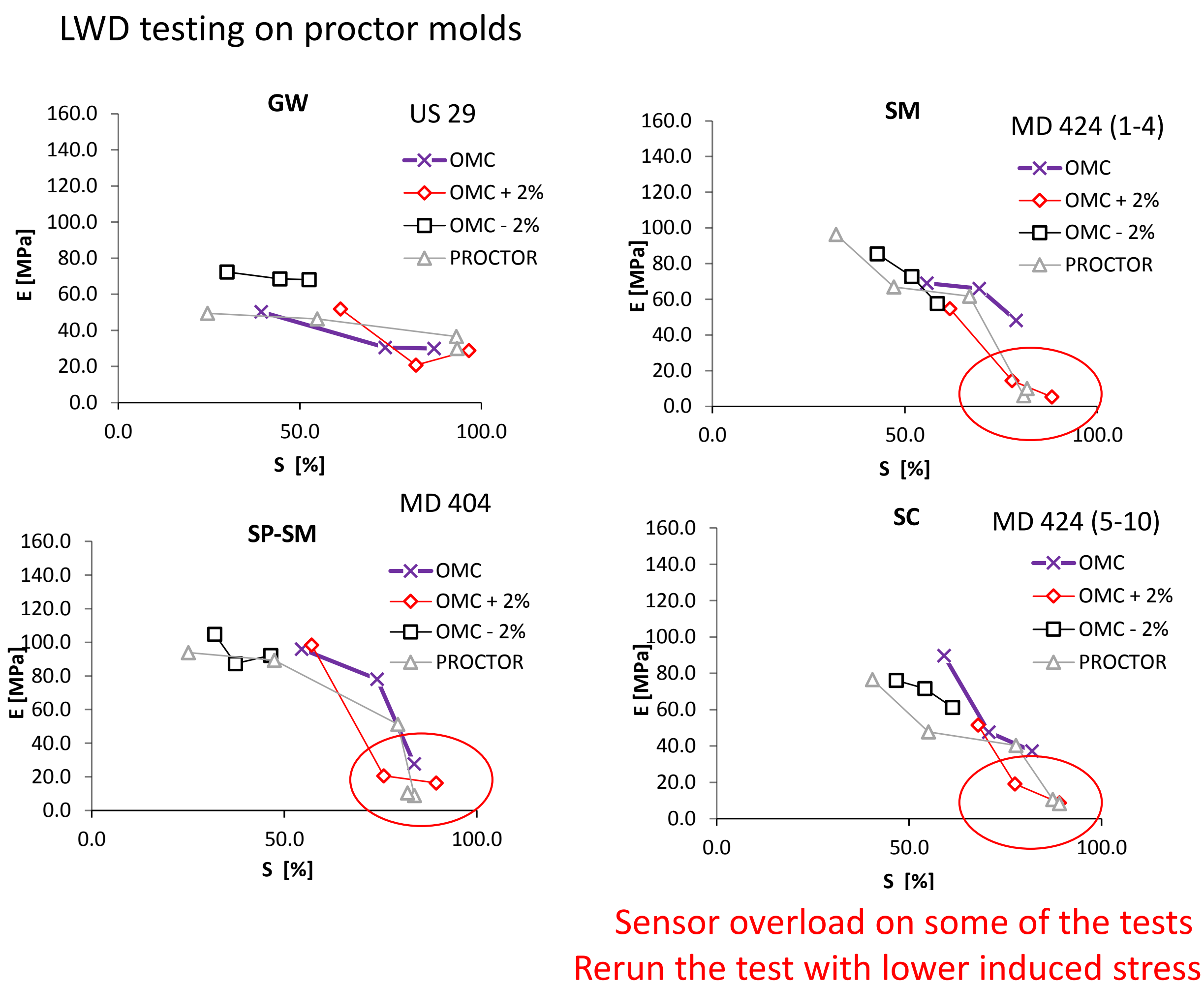

Figure 23. LWD tests on Proctor molds.

Summarized below are the detailed data from LWD tests performed on Proctor molds. The loads shown in red are the corrected loads based on the relationship from Figure 22. The peak deflections shown in red are the tests that mechanically bottomed the geophone.

GW		Force [N]	Disp. [mm]	stiffness [kN/mm]	Av. stiffness [kN/mm]	Moist. Cont. [%]
Proctor	PRCMF3	9355	2.230	4.195	10.1	2.8
		8411	0.874	9.624		
		8366	0.794	10.537		
		8522	0.876	9.728		
		8321	0.811	10.260		
		8391	0.809	10.372		
	PRCQ1	8554	1.320	6.480	9.5	5.2
		8416	0.929	9.059		
		8507	0.875	9.722		
		8509	0.965	8.818		
		8479	0.826	10.265		
		8458	0.902	9.376		
	PRCPF1	8595	1.940	4.430	7.5	7.5
		8794	1.270	6.924		
		8586	1.280	6.708		
		8531	1.220	6.993		
		8538	1.140	7.489		
		8533	1.070	7.975		
	PRCW1	9669	2.520	3.837	6.1	8.8
		9819	1.810	5.425		
		9902	1.670	5.929		
		9814	1.620	6.058		
		9932	1.610	6.169		
		9896	1.600	6.185		
Drying- Compacted@OMC	ENV1	9009.0	2.220	4.058	6.1	7.0
		9206.0	1.560	5.901		
		9095.0	1.500	6.063		
		9285.0	1.420	6.539		
		8900.0	1.300	6.846		
		10382.2	2.060	5.040		
	ENV3	9292.0	2.850	3.260	6.2	5.9
		8792.0	1.350	6.513		
		9011.0	1.410	6.391		
		8769.0	1.430	6.132		
		8746.0	1.420	6.159		
		8787.6	1.370	6.414		
	ENV5	9260.0	2.410	3.842	10.3	3.2
		8583.0	0.690	12.439		
		8645.0	0.820	10.543		
		8434.0	0.893	9.445		
		8690.0	0.862	10.081		
		8676.3	0.760	11.416		
Drying- Compacted@OMC+2%	LUC7	10068.0	2.440	4.126	5.9	9.0
		10052.0	1.880	5.347		
		10219.0	1.870	5.465		
		10165.0	1.780	5.711		
		10448.0	1.700	6.146		
		10441.0	1.770	5.899		
	LUC8	10077.0	3.430	2.938	4.3	7.6
		10880.0	2.650	4.106		
		11020.0	2.610	4.222		
		10841.0	2.560	4.235		
		11034.0	2.580	4.277		
		10995.0	2.570	4.278		
	LUC10	9099.0	4.110	2.214	10.6	5.7
		8570.0	1.080	7.935		
		8326.0	0.870	9.570		
		7959.0	0.792	10.049		
		8396.0	0.886	9.476		
		8140.3	0.659	12.352		
Drying- Compacted@OMC-2%	ENV1	8620.0	4.110	2.097	10.2	7.0
		7667.0	1.080	7.099		
		7755.0	0.870	8.914		
		7801.0	0.792	9.850		
		7744.0	0.886	8.740		
		7822.9	0.659	11.871		
	ENV3	8859.0	2.850	3.108	5.5	5.9
		7744.0	1.350	5.736		
		7690.0	1.410	5.454		
		7654.0	1.430	5.352		
		7649.0	1.420	5.387		
		7689.6	1.370	5.613		
	ENV5	8893.0	2.410	3.690	9.3	3.2
		8111.0	0.690	11.755		
		8063.0	0.820	9.833		
		7862.0	0.893	8.804		
		7694.0	0.862	8.926		
		7784.3	0.760	10.242		

SP-SM		Force [N]	Disp. [mm]	stiffness [kN/mm]	v. stiffnes [kN/mm]	Moist. Co [%]
Proctor	SAND1	8767	1.28	6.855	11.5	4.2
		8579	0.78	10.944		
		8516	0.83	10.213		
		8443	0.73	11.624		
		8346	0.75	11.188		
		8348	0.71	11.717		
	SAND2	8414	1.07	7.859	11.8	6.2
		7903	0.70	11.238		
		8013	0.77	10.471		
		7884	0.71	11.160		
		7905	0.65	12.089		
		7769	0.64	12.195		
	SAND3	8796	1.19	7.386	10.7	8.0
		8434	0.84	10.100		
		8321	0.86	9.681		
		8190	0.84	9.719		
		8192	0.75	10.859		
		7744	0.68	11.411		
	SAND14	12709.65	6.83	1.861		9.9
		12046.24	10.80	1.115		
		11561.46	4.19	2.759		
		11365.22	3.91	2.907		
		12761.91	8.65	1.475		
		12813.26	7.85	1.632		
	SAND15	11343.34	3.88	2.924		11.4
		12771.64	7.22	1.769		
		12744.9	7.03	1.813		
		11893.82	4.72	2.520		
		12785.14	7.34	1.742		
		11692.89	4.39	2.664		
Drying- Compacted@OMC	ENV7	9624.066	1.98	4.861	4.7	8.3
		9634.836	1.99	4.842		
		9482.396	1.85	5.126		
		9730.948	2.08	4.678		
		9438.185	1.81	5.214		
		10000.32	2.34	4.274		
	ENV9	10592.97	2.96	3.579	10.9	7.2
		8284.57	0.85	9.793		
		8114.738	0.72	11.349		
		8370.222	0.91	9.168		
		8191.614	0.77	10.583		
		7975.028	0.61	13.095		
	ENV12	10381.28	2.73	3.803	13.3	5.5
		8362.585	0.91	9.220		
		8164.324	0.75	10.842		
		8049.092	0.67	12.104		
		7940.447	0.58	13.620		
		7911.09	0.56	14.102		
Drying- Compacted@OMC+2%	LUCA1	11208.66	3.70	3.029	3.2	9.7
		11170.2	3.65	3.060		
		11060.1	3.51	3.151		
		11036.04	3.48	3.171		
		11027.98	3.47	3.178		
		10913.28	3.33	3.277		
	LUCA3	11068.08	3.52	3.144	3.8	8.4
		10276.64	2.62	3.922		
		10583.96	2.95	3.588		
		10257.37	2.60	3.945		
		10520.43	2.88	3.653		
		10456.01	2.81	3.721		
	LUCA5	11621.5	4.28	2.715	13.8	6.2
		8211.057	0.79	10.407		
		8087.222	0.69	11.653		
		8084.597	0.69	11.683		
		8064.889	0.68	11.913		
		7738.538	0.43	17.872		
Drying- Compacted@OMC-2%	LUCA2	8480.222	1.00	8.480	12.9	6.1
		8064.889	0.68	11.913		
		7998.897	0.63	12.757		
		7989.622	0.62	12.886		
		8056.994	0.67	12.007		
		7925.78	0.57	13.856		
	LUCA4	8054.36	0.67	12.039	12.4	4.9
		7949.77	0.59	13.474		
		8066.204	0.68	11.897		
		7993.598	0.62	12.831		
		8164.324	0.75	10.842		
		7945.776	0.59	13.536		
	LUCA6	8475.195	1.00	8.509	15.0	4.3
		7823.839	0.50	15.774		
		7786.017	0.47	16.637		
		7841.351	0.51	15.405		
		7762.983	0.45	17.213		
		8033.269	0.65	12.302		

SM		Force [N]	Disp. [mm]	stiffness [kN/mm]	Av. stiffness [kN/mm]	Moist. Cont. [%]
Proctor	SAND6	7640	0.668	11.430	14.6	5.9
		7925	0.672	11.797		
		7857	0.626	12.554		
		7832	0.568	13.782		
		7708	0.527	14.639		
		7685	0.504	15.242		
	SAND8	8540	1.131	7.549	13.1	7.7
		8140	0.727	11.202		
		8068	0.696	11.594		
		7896	0.609	12.968		
		7988	0.636	12.553		
		7927	0.576	13.761		
	SAND7	8717	1.405	6.205	11.4	9.8
		8122	0.823	9.866		
		8047	0.735	10.942		
		7914	0.673	11.764		
		7828	0.714	10.962		
		7712	0.671	11.489		
	SAND9	10117	3.935	2.571		11.9
		10450	2.859	3.656		
		10601	2.728	3.887		
		10816	2.880	3.756		
		11208	3.117	3.595		
		11258	2.957	3.807		
	SLYCY7	12467.98	5.950	2.095		15.2
		12170.18	5.240	2.323		
		12203.62	5.310	2.298		
		10502.11	2.860	3.672		
		11804.95	4.570	2.583		
		12324.25	5.580	2.209		
Drying- Compacted@OMC	ENV11	8752.232	1.22	7.174	9.5	10.7
		8444.97	0.97	8.688		
		8315.345	0.87	9.558		
		8173.429	0.76	10.755		
		8317.905	0.87	9.539		
		8505.314	1.02	8.339		
	ENV14	9762.658	2.11	4.627	12.6	9.3
		8243.372	0.81	10.127		
		8236.919	0.81	10.182		
		8109.503	0.71	11.406		
		7948.439	0.59	13.495		
		7996.248	0.63	12.794		
	ENV15	8691.185	1.17	7.428	13.2	7.6
		7868.232	0.53	14.874		
		8457.576	0.98	8.613		
		7977.683	0.61	13.057		
		7980.338	0.61	13.018		
		7941.78	0.58	13.599		
Drying- Compacted@OMC+2%	LUCA8	12410.9	10.000	1.241		12.9
		12196.65	10.500	1.162		
		11967.53	4.850	2.468		
		12598.13	6.360	1.981		
		12772.87	7.230	1.767		
		12591.14	9.460	1.331		
	LUCA10	11276.74	3.790	2.975	3.7	11.7
		10592.97	2.960	3.579		
		10428.12	2.780	3.751		
		10465.26	2.820	3.711		
		10734.54	3.120	3.441		
		10343.48	2.690	3.845		
	LUC1	8642.021	1.130	7.648	9.9	9.1
		7633.299	0.356	21.442		
		7775.184	0.460	16.903		
		8020.064	0.643	12.473		
		8269.143	0.834	9.915		
		8269.143	0.834	9.915		
Drying- Compacted@OMC-2%	LUCA7	8530.334	1.040	8.202	11.2	8.7
		8087.222	0.694	11.653		
		8081.972	0.690	11.713		
		7998.897	0.627	12.757		
		8256.267	0.824	10.020		
		8164.324	0.753	10.842		
	LUCA9	8297.405	0.856	9.693	14.1	7.6
		7976.356	0.610	13.076		
		7935.116	0.579	13.705		
		7881.645	0.539	14.623		
		7865.547	0.527	14.925		
		7992.273	0.622	12.849		
	LUCA12	8752.232	1.220	7.174	16.6	6.4
		7861.519	0.524	15.003		
		7775.184	0.460	16.903		
		7773.829	0.459	16.936		
		7811.697	0.487	16.040		
		7775.184	0.460	16.903		

SC		Force [N]	Disp. [mm]	stiffness [kN/mm]	Av. stiffness [kN/mm]	Moist. Cont. [%]
Proctor	SEC6	8441.185	0.969	8.711	14.6	7.6
		7944.444	0.586	13.557		
		7971.044	0.606	13.154		
		7861.519	0.524	15.003		
		7881.645	0.539	14.623		
		7900.393	0.553	14.286		
	SEC5	9015.425	1.440	6.261	9.4	9.6
		8395.631	0.933	8.999		
		8920.738	1.360	6.559		
		8555.281	1.060	8.071		
		8368.95	0.912	9.176		
		8156.512	0.747	10.919		
	SEC4	9482.396	1.850	5.126	8.1	11.7
		8555.281	1.060	8.071		
		8629.684	1.120	7.705		
		8542.817	1.050	8.136		
		8567.727	1.070	8.007		
		8542.817	1.050	8.136		
	SLYCY4	11328.67	3.860	2.935	3.0	13.8
		11386.93	3.940	2.890		
		11394.13	3.950	2.885		
		11336.02	3.870	2.929		
		11201.01	3.690	3.036		
		11154.69	3.630	3.073		
	SLYCY5	12811.62	8.040	1.593		15.4
		12519.15	6.100	2.052		
		12494.16	9.770	1.279		
		11647.72	4.320	2.696		
		12715.4	6.860	1.854		
		11458.11	4.040	2.836		
Drying- Compacted@OMC	ENV8	9371.324	1.750	5.355	7.7	11.8
		9062.331	1.480	6.123		
		9132.143	1.540	5.930		
		8441.185	0.969	8.711		
		8836.931	1.290	6.850		
		8654.339	1.140	7.592		
	ENV10	8080.659	0.689	11.728	12.8	10.3
		8039.865	0.658	12.219		
		8025.348	0.647	12.404		
		8010.809	0.636	12.596		
		7986.97	0.618	12.924		
	ENV13	7685.0	0.501	15.339	15.5	8.5
		7620.0	0.627	12.153		
		7678.0	0.560	13.711		
		7708.0	0.475	16.227		
		7717.0	0.468	16.489		
		7794.6	0.566	13.771		
Drying- Compacted@OMC+2%	LUCA11	11261.74	3.770	2.987		13.7
		11239.1	3.740	3.005		
		12703.73	6.800	1.868		
		11201.01	3.690	3.036		
		12811.35	8.050	1.591		
		11254.21	3.760	2.993		
	LUC2	11154.69	3.630	3.073	4.6	12.5
		9929.006	2.270	4.374		
		9980.034	2.320	4.302		
		9804.682	2.150	4.560		
		9730.948	2.080	4.678		
		9856.802	2.200	4.480		
	LUC3	11513.74	4.120	2.795	10.2	10.5
		8824.886	1.280	6.894		
		8190.316	0.773	10.595		
		8385.476	0.925	9.065		
		8135.648	0.731	11.129		
		8204.581	0.784	10.465		
Drying- Compacted@OMC-2%	LUC4	8642.021	1.130	7.648	11.7	9.8
		8063.573	0.676	11.928		
		8157.814	0.748	10.906		
		8113.429	0.714	11.363		
		7963.072	0.600	13.272		
		8216.235	0.793	10.361		
	LUC5	8991.862	1.420	6.332	13.9	8.5
		7977.683	0.611	13.057		
		7944.444	0.586	13.557		
		7909.754	0.560	14.125		
		8020.064	0.643	12.473		
		7853.456	0.518	15.161		
	LUC6	8325.58	0.878	9.482	15.1	7.3
		7960.413	0.598	13.312		
		7814.397	0.489	15.980		
		7833.272	0.503	15.573		
		7787.37	0.469	16.604		
		7965.73	0.602	13.232		

Effects of Saturation and Density on Resilient Modulus

In this study specimens were compacted using Standard and Modified compaction energies. Figure 24 shows the gradation and soil-water characteristic curve (SWCC) of the GW2 soil, respectively.

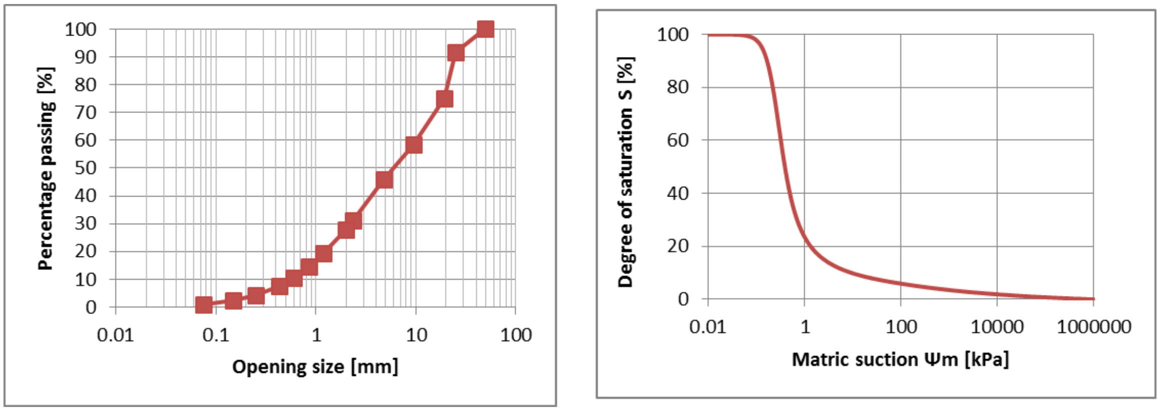

Figure 24. Gradation of GW2; SWCC of GW.

In the first two cases described below, the degree of saturation is the same between the two samples. For the first one (Figure 25) the degree of saturation is relatively high (S=76%) and therefore the associated suction is low. In such case, the effect of higher density is pronounced. The modified sample has higher modulus.

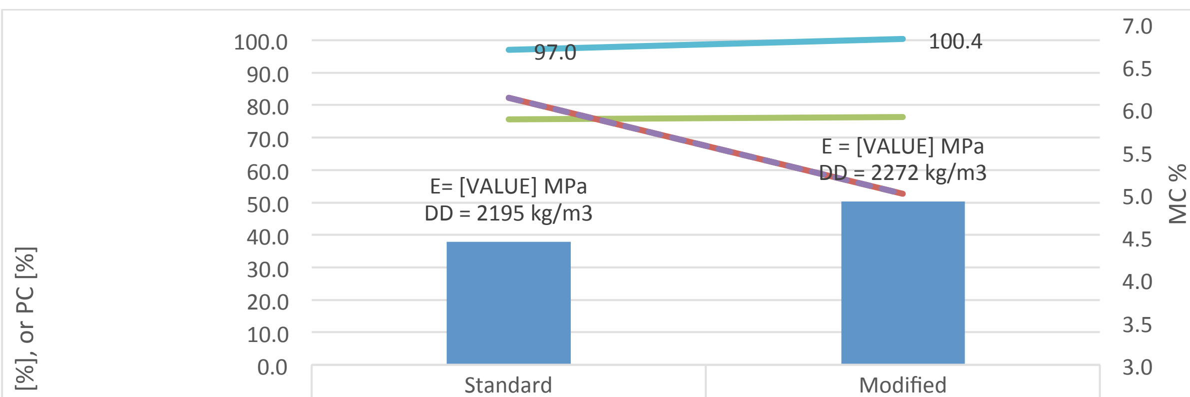

	Standard	Modified
E	37.9	50.3
S @testing	75.6	76.3
PC [%]	97.0	100.4
MC@Compaction	6.1	5.0
MC@Testing	6.1	5.0

Figure 25. Comparison of LWD modulus on Proctor mold for two specimens compacted using Modified and Standard compaction energies at similar saturation levels. High saturation level, S=76%.

In the second case (Figure 26, again the saturation level is the same but lower at S=55% and therefore specimens are relatively dry as compared to the previous case. In this case, the low S is the dominant factor in determining the modulus and the effect of density is overshadowed. The modulus of the two specimens are higher than the previous case but are similar to each other.

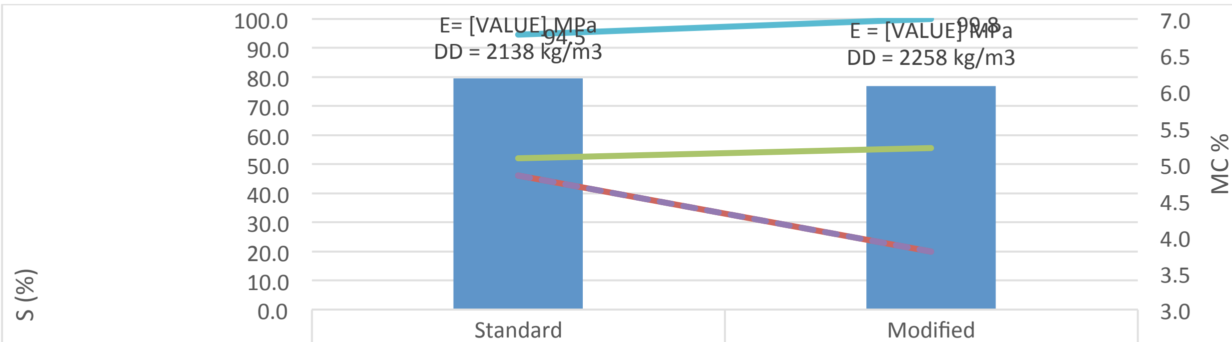

	Standard	Modified
E	79.5	76.7
S @testing	52.0	55.6
PC [%]	94.5	99.8
MC@Compaction	4.8	3.8
MC@Testing	4.8	3.8

Figure 26. Comparison of LWD modulus on Proctor mold for two specimens compacted using Modified and Standard compaction energy at similar saturation levels. Lower saturation level, S=55%

For the next two cases, the gravimetric moisture content was kept the same. In the first case at a higher gravimetric moisture content of around 5% (Figure 27), the specimen with higher S has the lower modulus even though its density is higher.

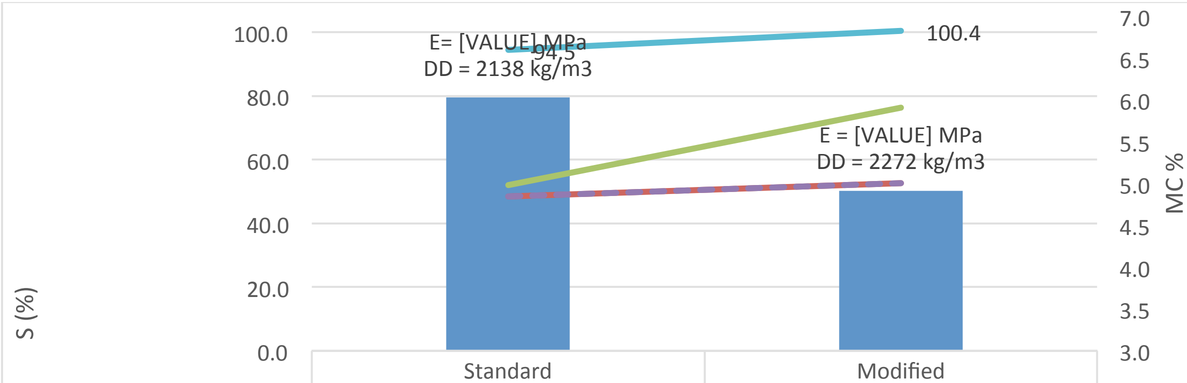

	Standard	Modified
E	79.5	50.3
S @testing	52.0	76.3
PC [%]	94.5	100.4
MC@Compaction	4.8	5.0
MC@Testing	4.8	5.0

Figure 27. Comparison of LWD modulus on Proctor mold for two specimens compacted using Modified and Standard compaction energies at similar gravimetric moisture contents. Higher moisture content, w=5%.

But in the next case at a slightly lower gravimetric water content of w=3.8%, the moduli are similar due to the counteracting effects of S and DD.

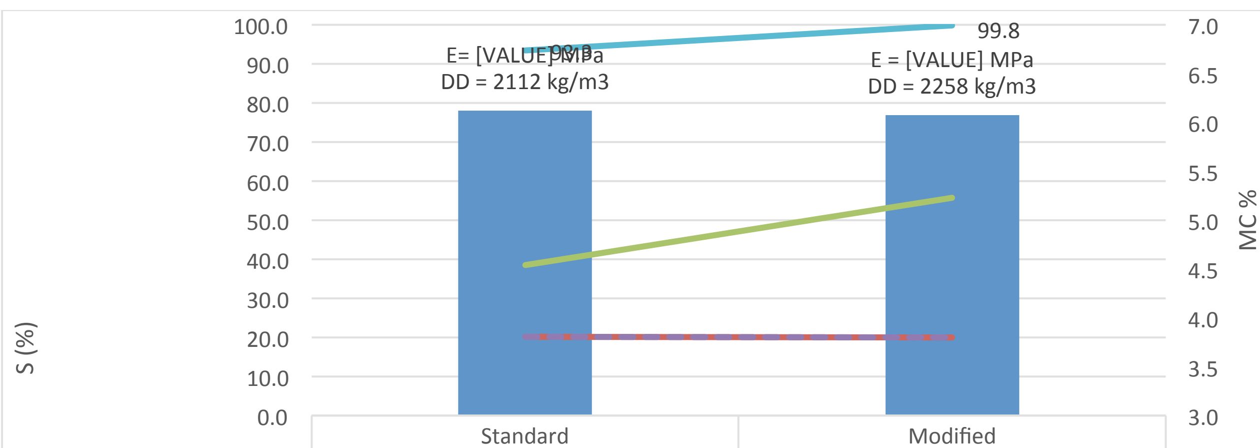

	Standard	Modified
E	77.9	76.7
S @testing	38.4	55.6
PC [%]	93.3	99.8
MC@Compaction	3.8	3.8
MC@Testing	3.8	3.8

Figure 28. Comparison of LWD modulus on Proctor mold for two specimens compacted using Modified and Standard compaction energies at similar gravimetric moisture contents. Lower moisture content, w=3.8%.

The following Table 4 summarizes all of the test results. It can be seen that for the modified compacted sample, the gain in modulus is significant when the specimen compacted at S=76.3% is dried to 67.8%. After drying to 67.8% percent its modulus (99.6 MPa) is much higher than specimen compacted at standard compaction effort at much lower degree of saturation of 38.4%. Therefore modulus is a combination of S and DD.

Table 4. Summary of test results.

	MC@ Compct	MC@ Test	DD	PC	e	S @comp	S @testing	E
	[%]	[%]	[kg/m3]	[%]	[%]	[%]	[%]	[MPa]
Stnd	5.2	5.2	2104.3	93.0	26.9	51.5	51.5	72.6
Stnd	4.9	4.9	2155.5	95.3	23.9	54.4	54.4	87.5
Stnd	4.5	4.5	2153.7	95.2	24.0	50.0	50.0	78.4
Stnd	3.8	3.8	2111.6	93.3	26.4	38.4	38.4	77.9
Stnd	3.8	3.3	2111.6	93.3	26.4	38.4	33.7	79.2
Stnd	6.1	6.1	2194.4	97.0	21.7	75.6	75.6	37.9
Stnd	6.8	6.8	2262.2	100.0	18.0	101.2	101.2	41.7
Mod	5.0	5.0	2271.9	100.4	17.5	76.3	76.3	50.3
Mod	5.0	4.4	2271.9	100.4	17.5	76.3	67.8	99.6
Mod	3.8	3.8	2258.4	99.8	18.2	55.6	55.6	76.7

Cary and Zapata has shown the simultaneous effect of DD and S on the environmental factor Fu. By plotting the contours of Fu versus DD and S graph we can obtain the combined effect of the two factors on modulus. This is shown in Figure 29.

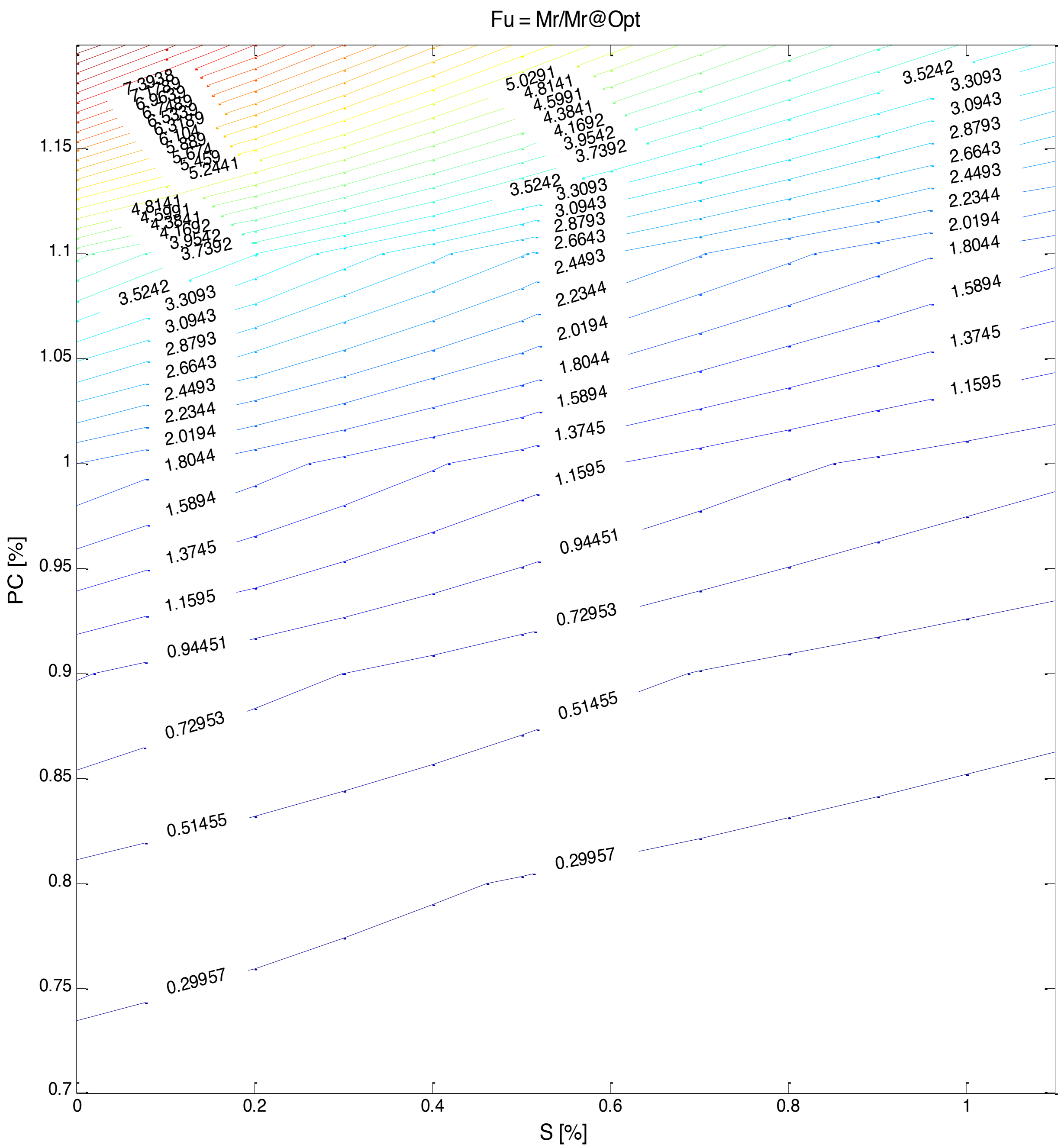

Figure 29. Contours of Fu vs. PC and S as predicted by Cary and Zapata model.

Appendix E: Test Pit Designs

The two test pits will be designed as follows:

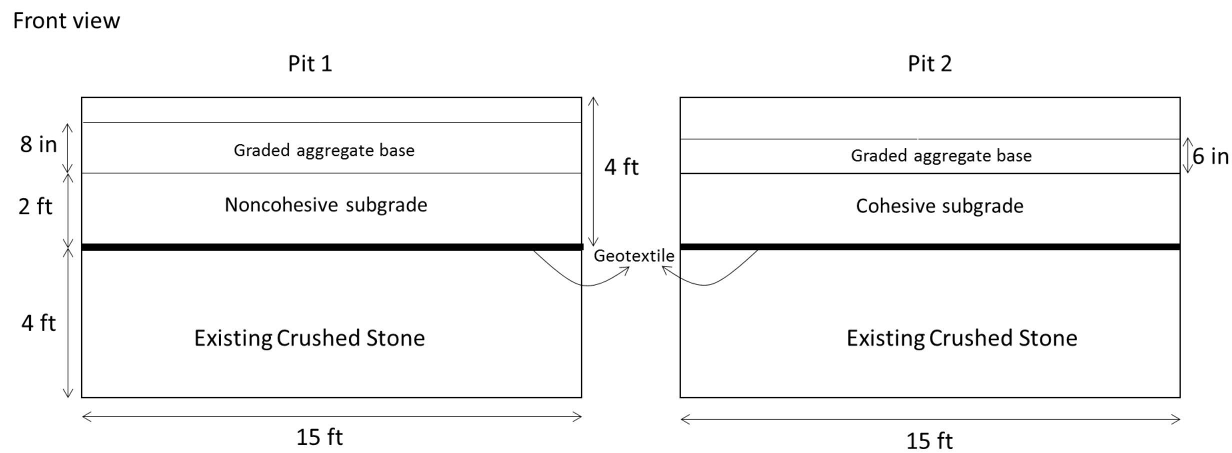

Priority Number 1:

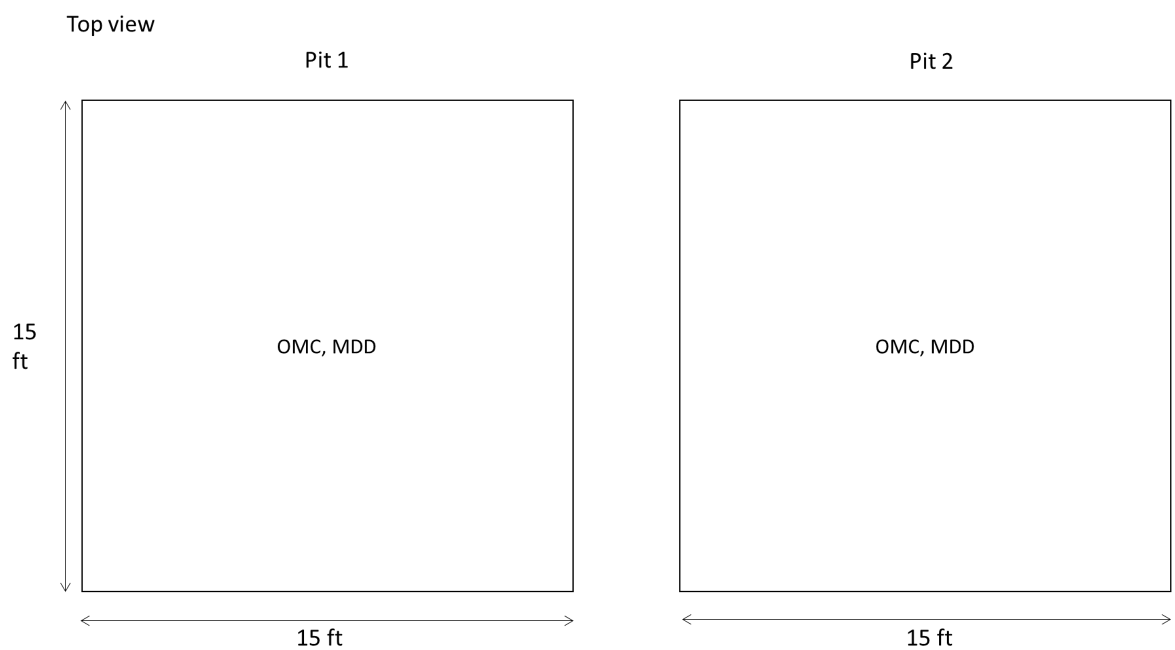

Priority Number 2:

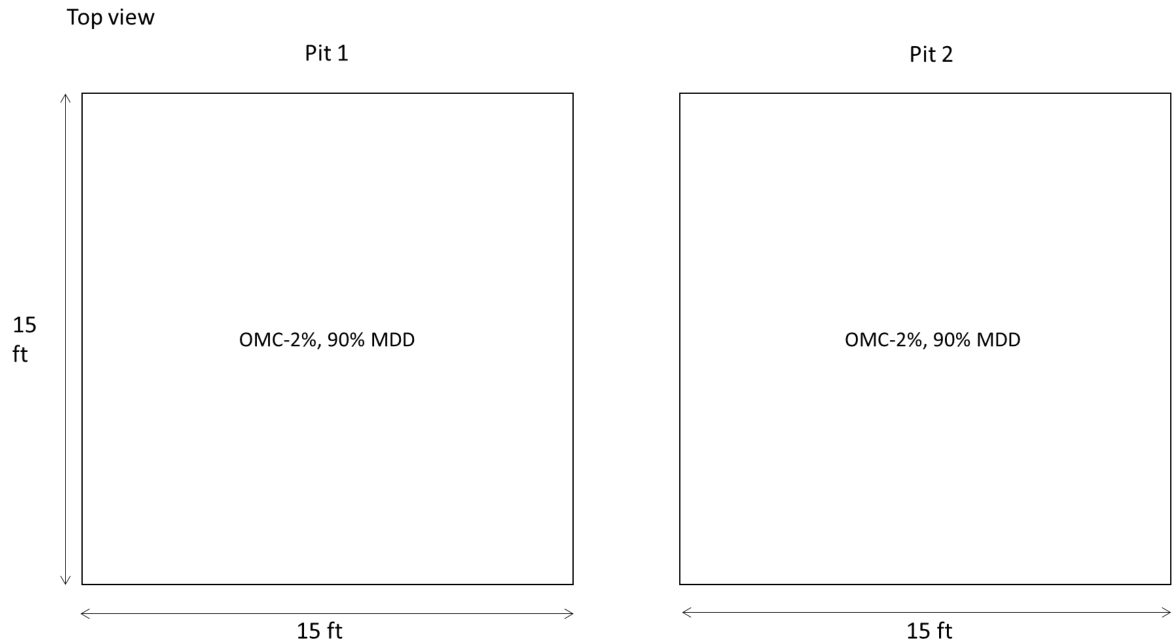

The reason for selection of the designs was to provide a cohesive and noncohesive subgrade, and sections that should "pass" the test and sections that should "fail" the LWD based specification. The sections will be instrumented with pressure gauges, strain gauges, thermometer, and moisture sensors to collect real time data during LWD testing.

Appendix F: Field Validation

Proceeding the online meeting with TAC the following field project information sheet has been sent to TAC to collect the best sites for validation of LWD QA procedure. To date we have received responses from Florida, Indiana, and New York.

Table 5. Field project information table.

Project Info	Site ID	
	Address	
	Construction Dates	
	Project Length	
	Agency Contact	
Layer thickness	Base	
	Sub-base	
Soil Classification	Base	
	Sub-base	
	Subgrade	
Local availability of test equipment	LWD-Zorn	
	LWD-Dynatest	
	Nuclear Gauge	
	Other equipment	
Comments		